4

Frequency UWB Channel

Gonzalo Llano, Juan C. Cuellar
and Andres Navarro
Universidad Icesi
Colombia

1. Introduction

Ultra wideband (UWB) transmission systems are characterized with either a fractional bandwidth of more that 20%, or a large absolute bandwidth (>500 MHz) in the 3.1 GHz to 10.6 GHz band, and for a very low power spectral density (−41.25 dBm/MHz, equivalent to 75nW/MHz), which allows to share the spectrum with other narrowband and wideband systems without causing interference (FCC, 2002), this spectral allocation has initiated an extremely productive activity for industry and academia.

Wireless communications experts now consider UWB as available spectrum to be utilized with a variety of techniques and not specifically related to the generation and detection of short RF pulses as in the past (Batra, 2004). For this reason, UWB systems are emerging as the best solution for high speed short range indoor wireless communication and sensor networks, with applications in home networking, high-quality multimedia content delivery, radars systems of high accuracy, etc. UWB has many attractive properties, including low interference to and from other wireless systems, easier wall and floor penetration, and inherent security due to its Low Probability Interception/Detection (LPI/D). Two of the most promising applications of UWB are High Data Rate Wireless Personal Area Network (HDR-WPAN), and Sensor Networks, where the good ranging and geo-location capabilities of UWB are particularly useful and of interest for military applications (Molisch, 2005).

Three types of UWB systems are defined by the Federal Communications Commission in United States: imaging systems, communication, measurement and vehicular radar systems. Currently the United States permits operation of UWB devices. In Europe a standardization mandate was forwarded to CEN/CENELEC/ETSI for harmonized standards covering UWB equipment (ECS, 2007), and regulatory efforts are studied by Japan (Molisch, 2005). In order to deploy UWB systems which carry out all those potentials, we need to analyze UWB propagation and the channel properties arising from this propagation, especially in the frequency domain. Given the large bandwidth (7.5 GHz) authorized for UWB and hence its low time resolution (133 ps), the conventional channel models developed to model the received envelope as a Rayleigh random variable in narrowband and wideband transmissions are inadequate in UWB signaling. Multipath fading resistance and high data rate transmission capacity, are the main characteristics of the UWB technology (Batra, 2004), render such UWB technology an excellent candidate for many indoor and short-range applications as compared to other wireless technologies. Applications of UWB can be found in high data rate wireless personal area networks, positioning, location and home network communications related to multimedia applications (Liuqing, 2007).

2. Statistical characterization of UWB channel

All wireless systems must be able to deal with the challenges of operating over a environment hostile, as the mobile wireless channel with multipath propagation channel, where objects in the environment cause multiple reflections to arrive at the receiver. As a result, the wireless systems will experience multipath fading, or amplitude fluctuations, resulting from the constructive or destructive combining of the reflected paths. Therefore an accurate channel model is needed to design a wireless system and to predict maximum ranges, power transmission, modulation schemes, rate coding, and transmission rates.

There are several ways to characterize a wireless channel: Deterministic and Statistical methods. When the channel is influenced by some unknown factor, exact prediction with deterministic models is not possible; in this case, statistical models are used. These statistical models are based on extensive measurements campaigns and they give us the channel behavior, especially, the received envelope and the path arrival time distribution.

To characterize the UWB channel using statistical methods, the IEEE 802.15 standardization group responsible for HDR-WPAN and Low Rate WPAN (LR-WPAN) organized two working groups: Task Group 3a (TG3a) and 4a (TG4a) to development an alternative physical layer based on UWB signaling (Molisch, 2005). IEE 802.15.3a TG3a proposed a channel model for HDR-WPAN applications (Foerster et al., 2003) and the TG4a a channel model for evaluation low rate applications proposed by the IEEE 802.15.4a standard (Mol05 et al., 2005)]. The TG4a model can be used in indoor and outdoor environments with longer operating range (i.e.,>10 m in indoor and up to few hundred meters for outdoor) and lower data rate transmission (between 1 kb/s and several Mb/s). There are two techniques signaling for this standard: a multiband orthogonal frequency division multiplexing (MB-OFDM) and a code-division multiple access (CDMA).

2.1 IEEE 802.15.3a channel model

To characterize the UWB channel for applications HDR-WPAN three indoor channel models have been proposed: the Rayleigh tap delay line model (same as the one used in 802.11 standard), Saleh-Valenzuela (S-V) (Saleh, 1987) and the Δ-K (Hashemi, 1993) models. The S-V and Δ-K models use a Poisson statistical process in order to model the arrival time of clusters (multipath components –MPC- which arrive from a same scatter). Nevertheless, the S-V model is unique in its approach of modeling the arrival time in cluster as well as MPC within a cluster. The S-V model defines that the multipath arrival times are random process based in Poisson distributions. Therefore the inter-arrival time of MPC are exponentially distributed, and defines four parameters to describe the channel: The cluster arrival rate (Λ), the path arrival rate (λ) within a cluster, the cluster decay time constant (η), path time constant (γ).

The principle of S-V channel is shown in the Fig.1. In this model, the small scale amplitude fading statistics follow a Rayleigh distribution and the power an exponential distribution, is defined by the cluster and ray decay factors.

However, measurements in UWB channels indicated that the small scale amplitude statistics denoted by α_{k1}, follow a lognormal or Nakagami-m distribution. The IEEE TG3a recommended using a lognormal distribution for the multipath gain magnitude. In this temporal model the power of the clusters and ray decays over time, this effect was modeled as an exponentially decaying power profile with increasing delay from the first path. Fig. 2

shows the temporal model of the 802.15.3a UWB channel. Based on these results, the SV model was modified for IEEE TG3a.

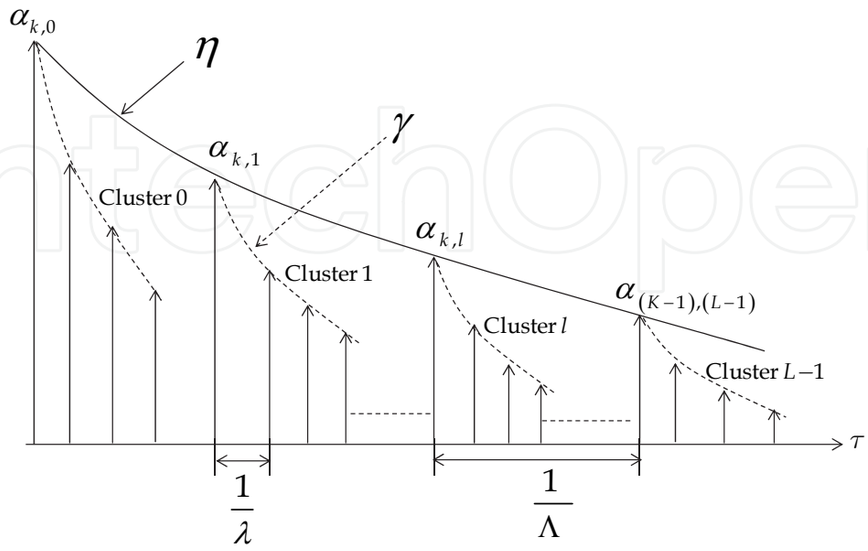

Fig. 1. Principle of the Saleh-Valenzuela Channel model

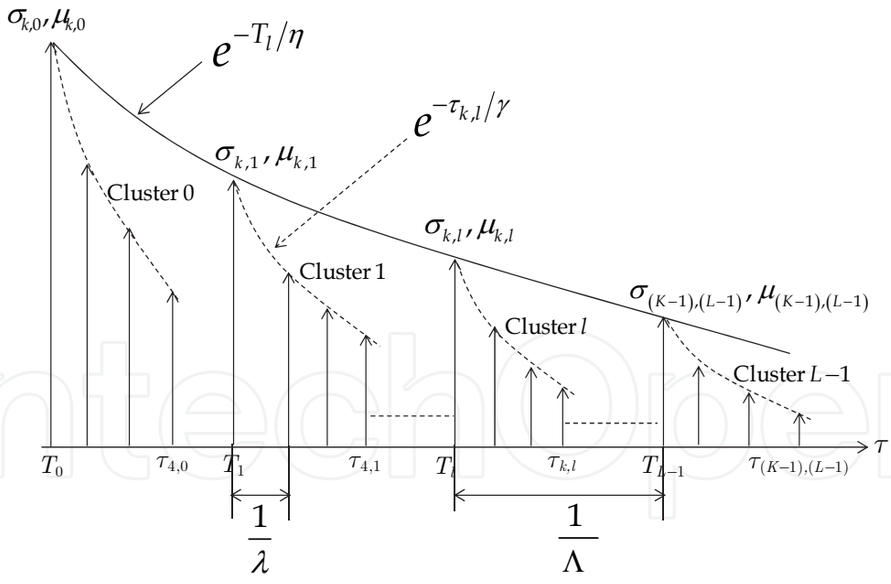

Fig. 2. Temporal model of IEEE 802.15.3a UWB Channel

The channel impulse response (CIR) time-variant for 802.15.3a UWB channel and denoted by $h(t;\tau)$, is given by (Foerster et al., 2003) as

$$h(t;\tau) = X(t)\sum_{l=1}^{L_C}\sum_{\substack{k=1 \\ l\neq k}}^{L_T}\xi_l(t)\beta_{k,l}(t)e^{j\varphi k,l(t)}\delta\left[\tau - T_l(t) - \tau_{k,l}(t)\right], \quad (1)$$

where, t represents the temporal variation of the channel due to motion of the receiver and τ the channel multipath delay. In addition, l represents the cluster index and k the MPC index within a lth cluster; L_c is the cluster numbers and L_r the rays numbers within the cluster (Multipath Components –MPC-), T_l is the arrival time of the lth cluster; and $\tau_{k,l}$ is the arrival time of the kth component inside the lth cluster. ξ_l is the amplitude of the lth cluster, $\beta_{k,l}$ is the amplitude of the kth path inside the lth cluster, $\varphi_{k,l} = 2\pi f_c \tau_{k,l}$, the phase of the path and $\delta(\bullet)$ the Kronecker delta function. $X(t)$ is a stochastic process that define the variations in the path gain amplitude due to non-line-of-sight (NLOS) propagation and characterize the slow fading (shadowing) and $\alpha_{k,l}(t)=\xi_l(t)\beta_{k,l}(t)$ is a stochastic processes that characterize the fast fading of the 802.15.3a UWB channel.

Let $\Delta\tau_{k,l} = \tau_{k,l} - \tau_{(k-1)l} = 1/W$, the width of the resolvable timebin, W the channel bandwidth, $N = \lceil L_c \times L_r \rceil = \lceil \tau_{\max}/\Delta\tau_{k,l} \rceil$ the number of timebins for the CIR of $h(t;\tau)$ defined in (1), $\tau_{\max}$ is the maximum excess delay of the channel and $\lceil \bullet \rceil$ is the ceiling function. If the nth timebin does not contain any MPC, then $\alpha_{k,l}(t)=\xi_l(t)\beta_{k,l}(t)=0$. Note, that in the Equation (1) the variation of the magnitude of the complex envelope due to slow fading or shadowing appears as a multiplier effect through the random variable (RV) $X = 10^{x/20}$, where x is a independent normal RV with zero mean and standard deviations σ_x(dB)=3 dB [Foe03], i.e., $x \sim \mathcal{N}(0,\sigma_x)$. Therefore, X is a independent lognormal RV with zero mean and standard deviation in nepers σ_X(Np), i.e., $X \sim \mathcal{L}(0,\sigma_X)$, where σ_X (Np)=[ln(10)/20]σ_x(dB). The amplitude of the envelope of the 802.15.3a UWB channel considering the slow fading and fast fading is calculated as

$$\Upsilon(t) = \left|h(t;\tau)\right| = X(t)\sum_{l=1}^{L_C}\sum_{\substack{k=1 \\ l\neq k}}^{L_r}\xi_l(t)\beta_{k,l}(t) \tag{2}$$

Since the two stochastic processes that characterize the fast fading and slow fading (shadowing) are independent, uncorrelated and static. The mean power of 802.15.3a UWB channel is given by

$$\Omega_\Upsilon \triangleq E\{\Upsilon^2\} = E\{X\}\sum_{l=0}^{L_C-1}\sum_{k=0}^{L_r-1}E\left\{\left|\xi_l\beta_{k,l}\right|^2\right\} = \bar{X}\sum_{l=0}^{L_C-1}\sum_{\substack{k=0 \\ l\neq k}}^{L_r-1}\Omega_{k,l}\,, \tag{3}$$

where, $E\{\cdot\}$ denote statistical expectation, $\Omega_{k,l}$ is the mean power of the kth MPC or path due to fast fading, $\bar{X}$ is the mean power due to shadowing and is given by

$$E\{X\} = \exp\left(\frac{\sigma_X^2}{2}\right) = \exp\left[\left(\frac{\ln(10)}{20}\right)^2\frac{\sigma_x^2(\mathrm{dB})}{2}\right], \tag{4}$$

Since σ_x(dB) = 3 dB, the average power variation due to shadowing is $\bar{X}$ = 1.04 dB. Applications using UWB systems are designed for indoor or outdoor environments, where the mobility of the TX/RX is very low. Therefore, the effect of temporal selectivity caused by either relative motion between the mobile and base station or by movement of objects in the channel which causes frequency shift by Doppler spread of the signal MB-OFDM in an UWB system, is very small compared with the bandwidth of UWB channel (1.584 GHz in

mode 1). Consequently 802.15.3a UWB channel is assumed time-invariant or static during the transmission of an OFDM symbol (Malik, 2008), i.e., $h(t;\tau) = h(\tau)$. Similarly, the channel is assumed Wide Sense Stationary (WSS), its mean energy remains constant during transmission of an MB-OFDM symbol, i.e., $m_{h(t;\tau)} \triangleq E\{h(t;\tau)\} = \text{Kte}$, and its autocorrelation function does not depend on the absolute momentos t_1 and t_2, depends on the difference between the two time points $\tau = t_1 - t_2$, i.e., $R_{h(t;\tau)}(t_1,\tau_1;t_2,\tau_2) \triangleq E\{h^*(t_1,\tau_1)h(t_2,\tau_2)\}$.
Hence, that we can assume the channel impulse response (CIR) of the indoor 802.15.3a UWB channel given by Eq. (1) as time-invariant, and only consider the dispersive effect of the channel denoted by variable, τ, therefore, the CIR of the UWB channel time-invariant is given by (Foerster at et., 2003) as

$$h(\tau) = \sum_{l=1}^{L_C} \sum_{\substack{k=1 \\ l \neq k}}^{L_T} \alpha_{k,l} e^{j\varphi_{k,l}} \delta(\tau - T_l - \tau_{k,l}) \tag{5}$$

The module $h(\tau)$ denoted by $\alpha_{k,l} = |h(\tau)|$, represent the gain magnitude due to the fast fading in UWB channel and is defined as a random variable (RV) that follow a lognormal distribution with mean $\mu_{k,l}$ and standard deviation $\sigma_{k,l}$, i.e., $\alpha_{k,l} \sim \mathcal{L}(\mu_{k,l},\sigma_{k,l})$. In the temporal model of 802.15.3a UWB channel, the mean power of the kth MPC or path is given by

$$\Omega_{k,l} = E\{\alpha_{k,l}^2\} = E\{|\xi_l \beta_{k,l}|^2\} = \Omega_0 \exp(-T_l/\eta)\exp(-\tau_{k,l}/\gamma), \tag{6}$$

where Ω_0 is the mean power of the first path inside the first cluster. The amplitudes of the contributions $|\xi_l \beta_{k,l}|$ are mutually independent RV and their phases $\varphi_{k,l}$ are uniformly distributed from 0 to 2π. The module of the amplitude of the paths follows a lognormal distribution, given by

$$|\xi_l \beta_{k,l}| = 10^{(\mu_{k,l}+n1+n2)/20} \rightarrow 20\log(\xi_l \beta_{k,l}) \sim \mathcal{N}(\mu_{k,l}, \sigma_c^2 + \sigma_r^2), \tag{7}$$

where n_1 and n_2 are independent normal RV with zero mean and standard deviations σ_c and σ_r, given by $n_1 \sim \mathcal{N}(0,\sigma_c)$ and $n_2 \sim \mathcal{N}(0,\sigma_r)$ and correspond to the fading on each cluster and path respectively; $\mathcal{N}(a,b)$ represents a Gaussian distribution with mean a and standard deviation b. The mean denoted by $\mu_{k,l}$, for the lognormal distribution of $|\xi_l \beta_{k,l}|$ is obtained from Eq. (6) and Eq. (7) as

$$\mu_{k,l} = \frac{10\ln(\Omega_0) - 10T_l/\eta - 10\tau_{k,l}/\gamma}{\ln(10)} - \frac{(\sigma_c^2 + \sigma_r^2)\ln(10)}{20}. \tag{8}$$

The distribution of the cluster arrival time and ray arrival time is exponential whose probability density function (PDF) is given by

$$p_T(T_l|T_{l-1}) = \Lambda \exp[-\Lambda(T_l - T_{l-1})],\ l > 0, \quad p_\tau(\tau_{k,l}|\tau_{(k-1),l}) = \lambda \exp[-\lambda(\tau_{k,l} - \tau_{(k-1),l})],\ k > 0 \tag{9}$$

Average arrival time between clusters and rays inside a cluster is obtained from Eq. (9) according to (Llano, et al., 2009) as

$$E\{T_l\} = \Lambda\int_0^{\infty} T_l \exp\left[-\Lambda(T_l)\right]dT_l = \frac{1}{\Lambda}; \quad E\{\tau_{k,l}\} = \lambda\int_0^{\infty} \tau_{k,l} \exp\left[-\lambda(\tau_{k,l})\right]d\tau_{k,l} = \frac{1}{\lambda}. \tag{10}$$

More details of the channel model parameters IEEE TG3a can be found in (Foerster, 2003).

2.2 IEEE 802.15.4a channel model

This model was developed by the IEEE 802.15.4a standardization group for UWB systems ranging with low rates transmission (Molisch et al., 2005). Such as in the 802.15.3a channel model, the impulse response (in complex baseband) is modeled for the IEEE 802.15.4a by a generalized SV model, denoted by $h(\tau)$, is given by (Molisch et al., 2005).

$$h(\tau) = \sum_{l=1}^{L_C}\sum_{\substack{k=1 \\ l\neq k}}^{L_T} \alpha_{k,l} e^{j\varphi k,l}\delta\left(\tau - T_l - \tau_{k,l}\right), \tag{11}$$

where l and k represent the cluster and ray indexes within the lth cluster, respectively; $\alpha_{k,l}$ and $\varphi_{k,l}$ correspond to the multipath gain coefficient and phases of the kth ray in the lth cluster, respectively; T_l is the arrival time of the lth cluster; and $\tau_{k,l}$ is the arrival time (in relation to T_l) of the kth ray in the lth cluster. The cluster arrival time and the ray arrival time within each cluster are modeled as a Poisson distribution with arrival rates Λ and λ, respectively, with $\lambda > \Lambda$. The MPCs amplitudes, $\alpha_{k,l}$, follow a Nakagami-m distribution and they are mutually independent RV. The phase terms $\varphi_{k,l}$ are uniformly distributed between 0 and 2π. In the channel model, the number of clusters, L_c, is a Poisson distributed RV with probability density function (PDF) given by (Molisch et al., 2005)

$$p_{L_C}(L_c) = \frac{\overline{(L_c)}^{L_C}}{L_c!}\exp\left(-\overline{L_c}\right), \; L_c > 0, \tag{12}$$

where $\overline{L_c}$ is the mean number of clusters. According to this model, the statistics of the cluster inter-arrival times are described by a negative exponential RV whose PDF can be written as (Molisch et al., 2005)

$$p_T\left(T_l \middle| T_{l-1}\right) = \Lambda\exp\left[-\Lambda\left(T_l - T_{l-1}\right)\right], \; l > 0. \tag{13}$$

Due to the discrepancy in the fitting for the indoor residential, and indoor and outdoor office environments the IEEE TG4a proposes to model ray arrival times with mixtures of two Poisson processes as follows

$$p_\tau\left(\tau_{k,l} \middle| \tau_{(k-1),l}\right) = \nu\lambda_1 \exp\left[-\lambda_1\left(\tau_{k,l} - \tau_{(k-1),l}\right)\right] + (1-\nu)\lambda_2 \exp\left[-\lambda_2\left(\tau_{k,l} - \tau_{(k-1),l}\right)\right], \; k > 0, \tag{14}$$

where ν is the mixture probability, λ_1 and λ_2 are the ray arrival rates. The mean time between rays arrives inside a cluster is obtained from Eq. (14) according to (Llano 2009) as

$$E\{\tau_{k,l}\} = \nu\lambda_1\int_0^{\infty} \tau_{k,l}\exp\left[-\lambda_1(\tau_{k,l})\right]d\tau_{k,l} + (1-\nu)\lambda_2\int_0^{\infty} \tau_{k,l}\exp\left[-\lambda_2(\tau_{k,l})\right]d\tau_{k,l} = \frac{\nu(\lambda_2 - \lambda_1) + \lambda_1}{\lambda_2\lambda_1} \tag{15}$$

Power delay profile (PDP) in the 802.15.4a UWB channel is exponentially distributed within each cluster and the power of each MPC denoted by $\Omega_{k,l}$, can be calculated as

$$\Omega_{k,l} = E\left\{\alpha_{k,l}^2\right\} = \Omega_l \frac{1}{\gamma_l\left[(1-\beta)\lambda_1 + \beta\lambda_2 + 1\right]} \exp\left(-\tau_{k,l}/\gamma_l\right), \tag{16}$$

where Ω_l is the integrated mean power of the lth cluster, and γ_l is the intra-cluster decay time constant. The mean power Ω_l of the lth cluster follows an exponential decay, and in agreement (Molisch et al., 2005) can be calculated as

$$10\log\left(\Omega_l\right) = 10\log\left[\exp\left(-T_l/\eta\right)\right] + M_{cluster}, \tag{17}$$

where T_l is the arrival time of the cluster given by Eq. (13). $M_{cluster}$ is a RV Gaussian distributed with standard deviation $\sigma_{cluster}$. The cluster decay rates γ_l depend linearly on the arrival time of the cluster and is expressed as $\gamma_l = k_l + \gamma_0$, where k and γ_0 are parameters of the model. Fig. 3 shows the 802.15.4a UWB channel model used in simulations to evaluate the response frequency.

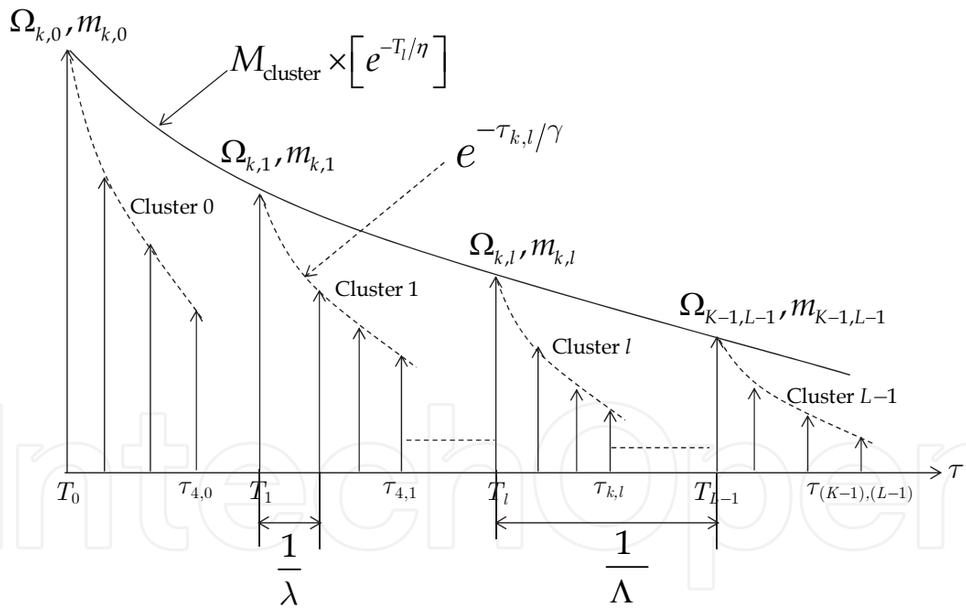

Fig. 3. Temporal model of IEEE 802.15.4a UWB Channel

In the 802.15.4a UWB channel model, the small scale fading for the multipath gain magnitude $\alpha_{k,l}$, is modeled as a Nakagami-m distribution whose probability density function (PDF) is given by (Nakagami, 1960)

$$f_{\alpha k,l}\left(\alpha_{k,l}\right) = \frac{2}{\Gamma\left(m_{k,l}\right)}\left(\frac{m_{k,l}}{\Omega_{k,l}}\right)^{mk,l} \alpha_{k,l}^{2mk,l-1} \exp\left(-\frac{m_{k,l}}{\Omega_{k,l}}\alpha_{k,l}^2\right), \quad m_{k,l} \geq 0.5, \tag{18}$$

where $m_{k,l}$ is the fading parameter of the kth path inside the lth cluster, $\Gamma(\bullet)$ is the gamma function and $\Omega_{k,l}$ is mean power of the kth path within the lth cluster given by Eq. (16). The $m_{k,l}$ parameter is modeled as a lognormal distributed RV, whose logarithm has a mean μ_m and standard deviation σ_m given by (Molisch et al., 2005)

$$\mu_m(\tau) = m_0 - k_m(\tau); \quad \sigma_m(\tau) = \hat{m}_0 - \hat{k}_m(\tau), \tag{19}$$

where $m_0, k_m, \hat{m}_0, \hat{k}_m$, are parameters of the model. More details of the channel model parameters IEEE TG4a can be found in (Molisch et al., 2005).

2.3 Frequency UWB channel

The studio of the UWB channel in frequency is of great interest to analyze the performance of the MB-OFDM UWB system concerning to the channel estimation, channel equalization, adaptive coding, bit and symbol error performance. Moreover, an accurate model in frequency of the UWB channel is required to design adaptive modulation and estimation channel techniques which increase the channel capacity. Frequency analysis of UWB channel and MB-OFDM signaling, with channel impulse response given by Eq. (5) and Eq. (11) shows that the amplitude of each subcarriers can be approximated by a Nakagami-m distribution and therefore its power is a Gamma distribution (Nakagami-m squared). In addition, this analysis enables to calculate the power correlation coefficient between a couple of subcarriers, important for the calculating the fade depth and fading margin due to small-scale fading. This analytical approach in frequency domain enables a proper evaluation of the link budget in terms of the bandwidth channel and it can be used to design and implement UWB communications systems.

2.3.1 Channel Transfer Function of the UWB channel

Hence, we will calculate the Channel Transform Function (CTF) through Fourier transform (FT) of the CIR given by Eq. (5). We will show that if the magnitude denoted by $|\xi_l \beta_{k,l}|$ in time of each of the 802.15.3a UWB channel contributions is modeled as a lognormal or Nakagami-m as the 802.15.4a, random variable (RV) and the number of MPC is high, the magnitude of the ith subcarrier denoted by $|H(f_i)| = r_i$, can be approximated by a Nakagami-m RV with equivalent fading parameter m_{eq}^i, and equivalent average power Ω_{eq}^i, (Llano, 2009) expressed as a function of the average time of arrival of the clusters, $1/\Lambda$, of the rays within a cluster, $1/\lambda$, decay rate of the cluster $1/\eta$, and rays $1/\gamma$. i.e., $r_i \sim \mathcal{M}\left(m_{eq}^i, \Omega_{eq}^i\right)$, where, $i = 0,1,\cdots,N_f$, and N_f defines the number of subcarriers in MB-OFDM UWB signaling. The Fourier transform of the CIR given by Eq. (5) and Eq. (11), denoted by $H(f_i)$, is expressed according to (Llano et al., 2009) as

$$\begin{aligned} H(f_i) &= \mathcal{F}\left\{h(\tau)\right\} = \int_{-\infty}^{\infty} h(\tau)\exp(-j2\pi f\tau)\,d\tau \\ &= \sum_{l=1}^{L_C}\sum_{\substack{k=1 \\ l\neq k}}^{L_T} \alpha_{k,l}\exp\left\{-j\left[2\pi f_i\left(T_l + \tau_{k,l}\right) - \varphi_{k,l}\right]\right\} = \sum_{l=1}^{L_C}\sum_{\substack{k=1 \\ l\neq k}}^{L_T} \alpha_{k,l}\exp\left[-j\left(\theta_{k,l}\right)\right] \end{aligned}, \tag{20}$$

where, $\alpha_{k,l}$ and $\theta_{k,l} = 2\pi f_i(T_l + \tau_{k,l}) - \varphi_{k,l}$, are the magnitude and phase respectively, at the ith subcarrier of the channel, and $\mathcal{F}\{\cdot\}$ Fourier transform operation. Let N_f be the number of

subcarriers or frequency points in the CTF, then $\Delta f = W/(N_f - 1) = 4.125$ MHz, is the frequency separation between subcarriers in a MB-OFDM UWB system. The magnitude $|H(f_i)|=r_i$, of the ith subcarrier in the frequency domain it is modeled as a Nakagami-m RV with probability density function (PDF) given by (Nakagami, 1960)

$$f_{|H(fi)|}(r_i) = \frac{2}{\Gamma(m_{eq}^i)}\left(\frac{m_{eq}^i}{\Omega_{eq}^i}\right)^{m_{eq}^i} r_i^{2m_{eq}^i-1}\exp\left(-\frac{m_{eq}^i}{\Omega_{eq}^i}r_i^2\right),\ m_{eq}^i \geq 0.5, \tag{21}$$

where Ω_{eq}^i, is the average power and m_{eq}^i, the fading parameter of the UWB channel.

2.3.2 Average power and fading parameter in frequency

The average power Ω_{eq}^i, and the fading parameter m_{eq}^i, of the ith subcarrier in UWB channel can be expressed according to (Nakagami, 1960) as

$$\Omega_{eq}^i \triangleq E\{r_i^2\} = E\left\{\left|H(f_i)\right|^2\right\} = E\left\{\left|H_R(f_i)\right|^2 + \left|H_I(f_i)\right|^2\right\}, \tag{22}$$

$$m_{eq}^i \triangleq \frac{\left(E\left\{\left|H(f_i)\right|^2\right\}\right)^2}{E\left\{\left|H(f_i)\right|^4\right\} - \left(E\left\{\left|H(f_i)\right|^2\right\}\right)^2}. \tag{23}$$

where, $|H_R(f_i)|$ and $|H_I(f_i)|$ are the real and imaginary part of the module $|H(f_i)|$ of the channel transfer function of the channel. The average power for the 802.15.4a UWB channel is obtained from Eq. (20) and Eq. (22) according to (Llano et al., 2009) as

$$\Omega_{eq}^i = \sum_{l=1}^{L_C}\sum_{\substack{k=1\\ l\neq k}}^{L_T} E\{r_i^2\} = \sum_{l=1}^{L_C}\sum_{\substack{k=1\\ l\neq k}}^{L_T}\Omega_{k,l} = \Omega_0\sum_{l=1}^{L_C}\sum_{\substack{k=1\\ l\neq k}}^{L_T}\exp\left[-\left(\frac{T_l}{\eta}+\frac{\tau_{k,l}}{\gamma}\right)\right]\times\frac{M_{\text{cluster}}}{\gamma\left[(1-\beta)\lambda_1+\beta\lambda_2+1\right]}. \tag{24}$$

The fading parameter m_{eq}^i, in frequency of the ith subcarrier of the 802.15.4a UWB channel, can be expressed according to (Llano at al., 2009) as

$$m_{eq}^i = \frac{\left(\sum_{l=1}^{L_C}\sum_{k=1}^{L_T}\Omega_{k,l}\right)^2}{\sum_{l=1}^{L_C}\sum_{k=1}^{L_T}\left(\frac{\Omega_{k,l}^2}{m_{k,l}}\right)+\sum_{l=1}^{L_C}\sum_{\substack{n=1\\ (l,k)\neq(n,m)}}^{L_C}\sum_{k=1}^{L_T}\sum_{m=1}^{L_T}\Omega_{k,l}\Omega_{m,n}}. \tag{25}$$

where, $\Omega_{k,l}$ is the mean power of the kth MPC or path given by Eq. (16) and $m_{k,l}$ is the fading parameter defined as a lognormal distributed RV, whit mean μ_m and standard deviation σ_m given by Eq. (19), i.e., $m_{k,l} \sim \mathcal{L}(\mu_m,\sigma_m)$. Fig. 4 shows the comparison of the amplitude $|H(f_i)|$ PDF of the 802.15.4a UWB channel, between the simulated data and the Nakagami-m analytical approximation, where Ω_{eq}^i, and m_{eq}^i, are calculated from Eq. (24) and Eq. (25). 8 clusters and 12 rays by cluster were assumed in simulations. The rest of parameters used in the Fig. 4 were: $\sigma_c = \sigma_r = 3.4$ dB, $\eta = 24$, $\gamma = 12$ and $\Omega_0 = 1$.

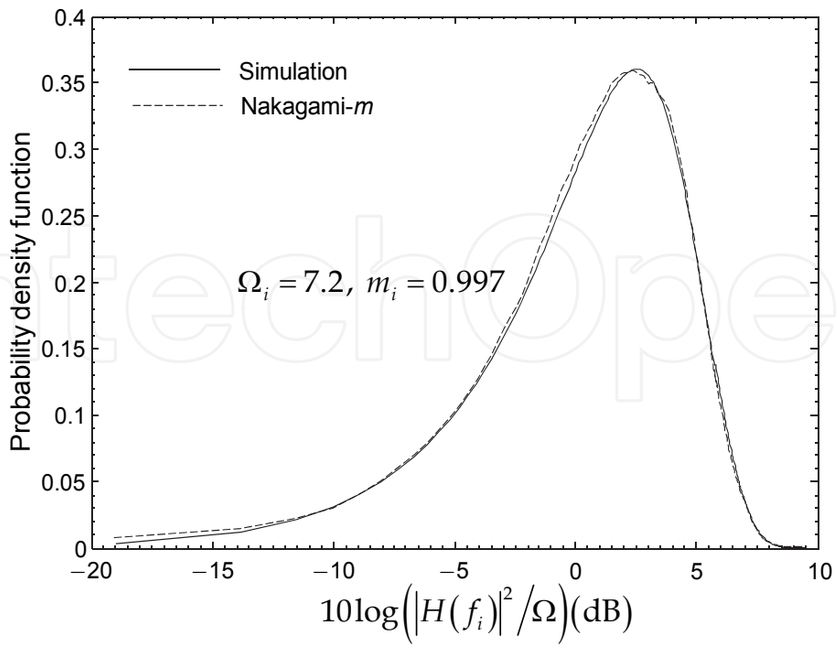

Fig. 4. Probability density function of the 802.15.4a UWB channel frequency amplitude $|H(f_i)|$ using the Nakagami-*m* analytical approximation

From Fig. 4, it can be observed that the Nakagami-*m* approximation and simulation curves are very similar and these results show that for a UWB channel with Nakagami-*m* fading and independents MPCs: a) the magnitude of the channel response frequency at each frequency bin is approximately Nakagami-*m* distributed with the mean power (Eq. (24)) and the fading parameter (Eq. (25)); and b) these results also show that if the MPC number is higher that 96 (number of rays multiplied by number of clusters) then the relative error in the m_{eq}^i, is less than 0.1% with respect to m_{eq}^i =1 (Rayleigh fading). The Mean Squared Error (MSE) between the data simulated and Nakagami-*m* PDF analytical expression given by Eq. (21) in Fig. 4 is de 0.16%. MSE is calculated as

$$\mathrm{MSE} = E\left\{\frac{1}{N}\sum_{n=1}^{N}\left(r_n - \hat{r}_n\right)^2\right\}, \tag{26}$$

where, r_n represent the analytical value obtained in the Eq. (21), $\hat{r}_n$ the value simulated and N the samples number. Fig. 5 shows the cumulative distribution function (CDF) for the amplitude $|H(f_i)|$ of channel response frequency normalized by the mean power Ω_{eq}^i. Note that $|H(f_i)|$ becomes Rayleigh distributed for a sufficiently high number of MPC (typical environment in UWB channels). For instance, if the MPC number is higher than 63 contributions then the difference of the CDF for 10^{-3} between the simulated distribution and the Rayleigh distribution is less than 2 dB.

2.3.3 Power correlation coefficient

As mentioned above, calculating the power correlation coefficient is important for evaluation of the fade depth and fade margin due to small-scale fading and allows a proper

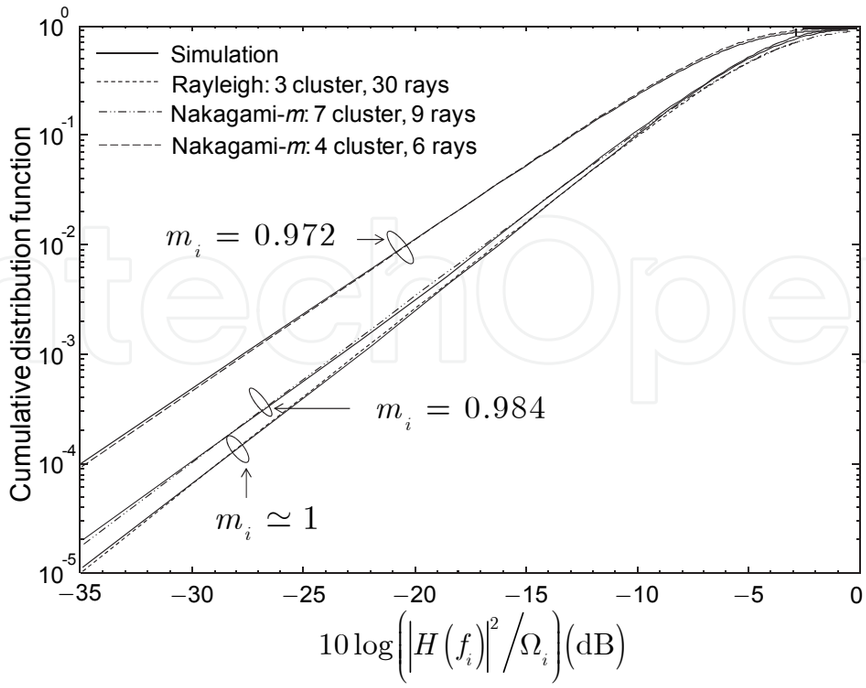

Fig. 5. Cumulative distribution function of the normalized channel frequency amplitude $|H(f_i)|$, using the Nakagami-*m* analytical approximation, for several MPC contributions.

evaluation of the link budget in terms of the bandwidth channel. In addition, as shown later, this analysis enable to calculate and validate through simulation the coherence bandwidth and coherence time of the MB-OFDM UWB channel. The power correlation coefficient $\rho_{i,j}$ in frequency of the UWB channel between the *i*th and *j*th subcarrier is defined according to (Papoulis, 2002) as

$$\rho_{ij} \triangleq \frac{\mathrm{cov}\left\{r_i^2 r_j^2\right\}}{\sqrt{\mathrm{var}\left\{r_i^2\right\}\mathrm{var}\left\{r_j^2\right\}}} = \frac{E\left\{r_i^2 r_j^2\right\} - E\left\{r_i^2\right\}E\left\{r_j^2\right\}}{\sqrt{\mathrm{var}\left\{r_i^2\right\}\mathrm{var}\left\{r_j^2\right\}}}, \tag{27}$$

where, $r_i = |H(f_i)|$, defines the amplitude of the *i*th subcarrier in frequency, and is approximated by a Nakagami-*m* distribution, therefore its power denoted by $r_i^2 = \left|H\left(f_i\right)\right|^2$ is a Gamma distribution and var(·) is the variance of the RV. The variance of the power $r_i^2 = \left|H\left(f_i\right)\right|^2$, of the *i*th subcarrier is given according to (Papoulis, 2002) as

$$\mathrm{var}\left\{r_i^2\right\} \triangleq \mathrm{var}\left\{\left|H(f_i)\right|^2\right\} = E\left\{\left|H(f_i)\right|^4\right\} - E^2\left\{\left|H(f_i)\right|^2\right\}. \tag{28}$$

The *n*th moment of the Nakagami-*m* distribution is given by (Nakagami, 1960)

$$E\left\{r^n\right\} = \frac{2}{\Gamma(m)}\left(\frac{m}{\Omega}\right)^m \int_0^\infty r^{2m+n-1}\exp\left(-\frac{mr^2}{\Omega}\right)dr = \frac{\Gamma\left(m+\frac{n}{2}\right)}{\Gamma(m)}\left(\frac{\Omega}{m}\right)^{\frac{n}{2}}, \tag{29}$$

where, *n* is a natural number. Evaluating Eq. (28) considering Eq. (29) is obtained

$$\mathrm{var}\left\{r_i^2\right\} = E\left\{\left|H(f_i)\right|^4\right\} - E^2\left\{\left|H(f_i)\right|^2\right\} = \frac{\Gamma\left(m_{eq}^i+2\right)}{\Gamma\left(m_{eq}^i\right)}\left(\frac{\Omega_{eq}^i}{m_{eq}^i}\right)^2 - \left[\frac{\Gamma\left(m_i+1\right)}{\Gamma\left(m_{eq}^i\right)}\left(\frac{\Omega_{eq}^i}{m_{eq}^i}\right)\right]^2 = \frac{\left(\Omega_{eq}^i\right)^2}{m_{eq}^i}. \quad (30)$$

Since the indoor UWB channel is assumed static during the transmission of an OFDM symbol, then the equivalent average power $\Omega_{eq}^i(i=1,\cdots,N_f)=\Omega$ and the equivalent fading parameter, $m_{eq}^i(i=1,\cdots,N_f)=m$. Substituting Eq. (30) in Eq. (27) is obtained $\rho_{i,j}$ as

$$\rho_{ij} \triangleq \frac{E\left\{r_i^2 r_j^2\right\} - \Omega_{eq}^i \Omega_{eq}^i}{\sqrt{\frac{\left(\Omega_{eq}^i\right)^2}{m_{eq}^i} \times \frac{\left(\Omega_{eq}^j\right)^2}{m_{eq}^j}}} = \left(\frac{E\left\{r_i^2 r_j^2\right\} - \Omega^2}{\Omega^2}\right) m. \quad (31)$$

Solving from Eq. (31) $E\left\{r_i^2 r_j^2\right\}$ in the numerator, is obtained according to (Llano et al., 2009)

$$E\left\{r_i^2 r_j^2\right\} = \sum_{l=1}^{L_C}\sum_{k=1}^{L_T}\left(\frac{m_{k,l}+1}{m_{k,l}}\right)\Omega_{k,l}^2 + \sum_{l=1}^{L_C}\sum_{\substack{k=1\\ l\neq k}}^{L_T}\sum_{n=1}^{L_C}\sum_{\substack{m=1\\ n\neq m}}^{L_T}\Omega_{m,n}\Omega_{k,l}\left[1+\cos\left(B_{l,n}^{k,m}\right)\right], \quad (32)$$

where, $B_{l,n}^{k,m} = 2\pi f\left[\left(T_l+\tau_{k,l}\right)-\left(T_n+\tau_{m,n}\right)\right]\left(i-j\right)$. Substituting Eq. (32) in Eq. (31) considering Eq. (24) and Eq. (25), one can be obtain a closed-form general expression of the power correlation coefficient for MB-OFDM UWB channel in frequency according to (Llano et al., 2009) as

$$\rho_{ij} = \frac{\sum_{l=1}^{L_C}\sum_{k=1}^{L_T}\left(\frac{\Omega_{k,l}^2}{m_{k,l}}\right) + \sum_{l=1}^{L_C}\sum_{\substack{k=1\\ l\neq k}}^{L_T}\sum_{n=1}^{L_C}\sum_{\substack{m=1\\ n\neq m}}^{L_T}\Omega_{m,n}\Omega_{k,l}\cos B_{l,n}^{k,m}}{\sum_{l=1}^{L_C}\sum_{k=1}^{L_T}\left(\frac{\Omega_{k,l}^2}{m_{k,l}}\right) + \sum_{l=1}^{L_C}\sum_{\substack{k=1\\ (l,k)\neq(n,m)}}^{L_T}\sum_{n=1}^{L_C}\sum_{m=1}^{L_T}\Omega_{m,n}\Omega_{k,l}}. \quad (33)$$

Note, that the power correlation coefficient given by the equation (33) is function of frequency separation between subcarriers, $\Delta f = f_1 - f_2 = W/(N_f - 1) = 4.125$ MHz, where W is the channel bandwidth in UWB system (W = 7.5 GHz), N_f = 128, is the number subcarriers in MB-OFDM UWB, and $\Delta_\tau = \left(T_l+\tau_{k,l}\right)-\left(T_n+\tau_{m,n}\right)$ the time delay of all multipath components (MPC) in the receiver. Particularizing Eq. (33) for the 802.15.3a MB-OFDM UWB channel is obtained to according (Llano et al., 2009)

$$\rho_{ij} = \frac{K\sum_{l=1}^{L_C}\sum_{k=1}^{L_T}\Omega_{k,l}^2 + \sum_{l=1}^{L_C}\sum_{\substack{k=1\\ l\neq k}}^{L_T}\sum_{n=1}^{L_C}\sum_{\substack{m=1\\ n\neq m}}^{L_T}\Omega_{m,n}\Omega_{k,l}\cos B_{l,n}^{k,m}}{K\sum_{l=1}^{L_C}\sum_{k=1}^{L_T}\Omega_{k,l}^2 + \sum_{l=1}^{L_C}\sum_{\substack{k=1\\ (l,k)\neq(n,m)}}^{L_T}\sum_{n=1}^{L_C}\sum_{m=1}^{L_T}\Omega_{m,n}\Omega_{k,l}}. \quad (34)$$

with, $A = \exp\left(4\sigma_{np}^2\right) - 2$ and σ_{np} the standard deviation of the lognormal fading in nepers units, given by

$$\sigma_{np} = \frac{\ln(10)}{20}\sqrt{\sigma_c^2 + \sigma_r^2}, \quad (35)$$

where, σ_c and σ_r are the standard deviations in dB units of clusters and rays, respectively. Fig. 6 shows the comparison of the correlation coefficient between simulated data and the analytical expression given by Eq. (34) for the following parameters: $\sigma_c = \sigma_r = 3.4$ dB, $\eta = 24$, $\gamma = 12$, $\Omega_0 = 1$, $L_c = 8$ and $L_r = 12$.

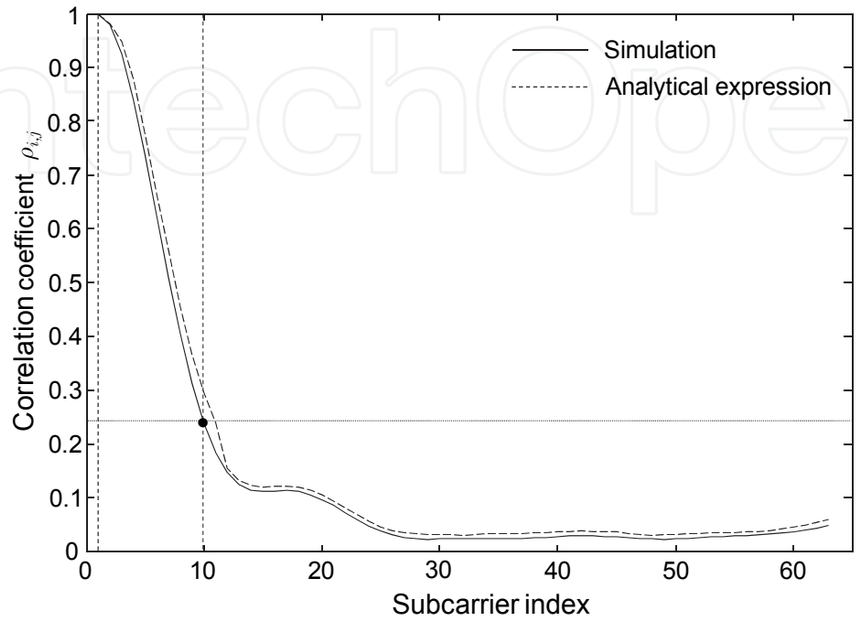

Fig. 6. Correlation coefficient as a function of the subcarrier order with respect to the first subcarrier position in the IEEE 802.15.3a MB-OFDM UWB channel type CM4.

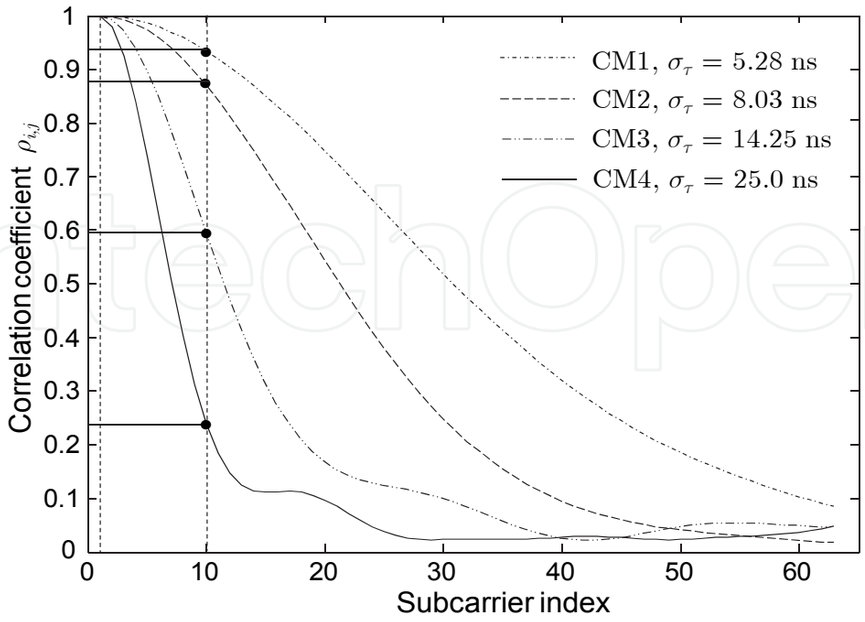

Fig. 7. Correlation coefficient as a function of the subcarrier order and delay spread in the 802.15.3a MB-OFDM UWB channel.

Note that for the maximum frequency separation between two pilot tones in MB-OFDM UWB channel defined as 9×4.125 MHz = 37.125 MHz, the correlation coefficient $\rho_{i,j}$ between the first (pilot) and tenth subcarrier is in a range from 0.25 to 0.98 for UWB channel CM4. Fig. 7 shows the correlation coefficient as a function of the UWB channel delay spread σ_τ, for four channel scenarios: CM1(σ_τ = 5.28 ns), CM2(σ_τ =8.03 ns), CM3(σ_τ =14.25 ns), and CM4(σ_τ = 25 ns). From this figure, we can observe a high dependence of the correlation coefficient between a couple of subcarriers on the delay spread. The parameters used in the simulations are given by (Foerster, 2003).

2.3.4 Coherence bandwidth of the MB-OFDM UWB channel

In this section we calculate the coherence bandwidth of UWB channel from the correlation coefficient $\rho_{i,j}$. The coherence bandwidth B_C is a parameter used to characterize the wireless channel in frequency domain, and can be defined as the range of frequencies over which the channel equally affects all spectral components of the transmitted signal, In other words, its transfer function $H(f,t)$ remains constant during transmission of an MB-OFDM symbol. Hence, the channel can be considered flat in frequency, i.e., passes all spectral components with approximately equal gain and linear phase. When the bandwidth of the transmitted signal B_S, is higher than the coherence bandwidth B_C, then the channel is frequency selective, which means that some spectral components of the signal B_S, will be modified quite differently by the channel, producing distortion in the received signal.

From Eq. (33) we find an expression to calculate the coherence bandwidth B_C. Let $A=\sum_{l=1}^{L_C}\sum_{k=1}^{L_r}\left(\frac{\Omega_{k,l}^2}{m_{k,l}}\right)$ and, $B=\sum_{l=1}^{L_C}\sum_{k=1}^{L_r}\sum_{n=1}^{L_C}\sum_{m=1}^{L_r}\Omega_{k,l}\Omega_{m,n}$. After simple algebraic operations, an expression is defined for frequency separation Δf of UWB channel in function of $\rho_{i,j}$ according to (Llano et al., 2009) as

$$B_C=\Delta f=\frac{\arccos\left[\frac{A\left(\rho_{ij}-1\right)}{B}+\rho_{ij}\right]}{2\pi\Delta\tau}. \tag{36}$$

Note which Eq. (36) aggress with [Fle96, Eq. (5)]. When $\rho_{i,j}$ = 1, corresponds to the highest correlation in frequency, in this case the coherence bandwidth $B_C = \Delta f = 0$ (represents the same frequency bin, $f_i = f_j$). When $\rho_{i,j} \to 0$, the temporal bins are widely separated and $\Delta\tau \to \sigma_\tau$ Then

$$B_C=\Delta f\simeq\frac{1}{4\sigma_\tau}. \tag{37}$$

Fig. 8 shows the simulation of the coherence bandwidth B_C defined in (36) as a function of delay spread for UWB channel. Note, that for $\rho_{i,j}$ = 0.75, B_C = 4.7 MHz, this value agrees with coherence bandwidth obtained in the measurement campaign for the indoor UWB channel carried out in the iTEAM of the Polytechnic University of Valencia (Spain) (Diaz 2007).

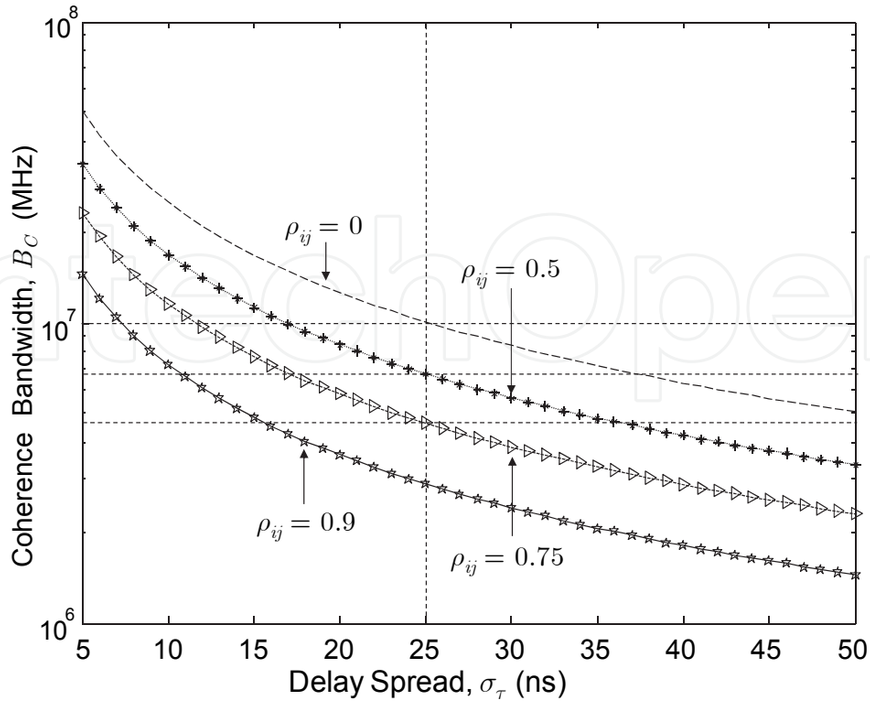

Fig. 8. Coherence bandwidth of the UWB channel as a function of delay spread

2.3.5 Coherence time of the MB-OFDM UWB channel

Delay spread, σ_τ, and *coherence bandwidth* B_C, are parameters which describe the time dispersive of the wireless channel in a local area, sufficient to characterize a static wireless channel. However, they do not offer information about the time varying of the channel in a small-scale region, caused by either relative motion between the mobile and base station or by movement of objects in the channel (Rappaport, 1996). To model the dynamic characteristic of the wireless channel, two parameters are defined: *Doppler spread* denoted by f_D and *coherence time* by T_C.

Doppler spread f_D is a measure of the spectral broadening caused by the time rate of change of the mobile radio channel. Coherence time T_C is the time domain dual of Doppler spread and are inversely proportional to one another.

Coherence time T_C for the UWB channel can be derived from Eq. (33). Defining $\Delta f = f_D$ and $\Delta\tau \rightarrow \sigma_\tau$, resulting

$$T_C = \frac{\arccos\left[\dfrac{A\left(\rho_{ij}-1\right)}{B}+\rho_{ij}\right]}{2\pi f_D}. \tag{37}$$

According to Eq. (37) when $f_D \rightarrow 0$, the wireless channel can be assumed static, because T_C, is high compared with the time transmission of a data frame in MB-OFDM UWB. Fig. 9 shows the simulation of the coherence time T_C derived in Eq. (37) as a function of Doppler spread for UWB channel. Note that for f_D = 13.2 Hz, T_C = 13 ms. The time transmission of a data

frame in MB-OFDM UWB is 0.63 ms (ECM, 2008). That is, it can transmit up to 22 data frames in the coherence time T_C = 13 ms.

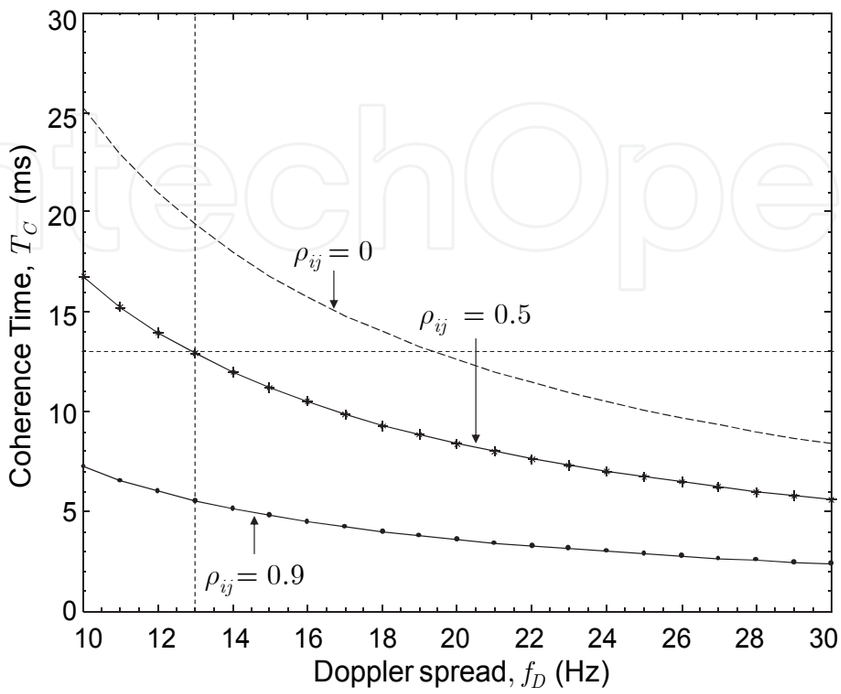

Fig. 9. Coherence time of the UWB channel as a function of Doppler spread

2.4 UWB channel power variation

The development of UWB communications systems requires a proper channel power characterization related to the propagation environment. Given the wideband nature of the UWB signal (bandwidth of 7.5 GHz), it is of paramount importance to characterize the channel power variations in terms of the channel bandwidth in order to evaluate the performance of UWB applications. It is well known that in wireless channels the multipath propagation causes destructive signal interference leading to small-scale fading. In an unresolved multipath components (MPCs) channel, the received signal can suffer severe fading increasing the system outage probability and degrading its performance (Jakes, 1974). In view of the fact that multipath propagation can produce received signal fade, it is necessary to provide additional power in the link budget to enhance the system quality. This additional power is known as fade margin (Cardoso, 2003). Other parameter to understand the small-scale fading concept is the fade depth that is referred to the received signal power variations about its local mean (Yang, 1999).

In order to have a complete description of the link budget and to define accurately the receiver sensitivity, a proper characterization of the channel power behavior is necessary. In this sense, the fade depth, the fade margin and the average power are important parameters to obtain an adequate description of the link budget, because they condition the final outage probability, and their knowledge is very useful to the radio network planning [Jak74]. It is well known that the fade depth and the fade margin depend on the channel bandwidth, the transmitted-received distance (Bastidas, 2005), and the small-scale fading conditions.

Therefore, their dependence is closely related to the environment where the propagation occurs. Due to the importance of these parameters in the radio network planning, they have been extensively analyzed in the literature, especially in narrowband channels. In (Cardoso, 2003), the fade depth and fade margin are evaluated for a Rician channel as a function of the equivalent received bandwidth, showing that the fade margin variation is related to the channel bandwidth and that it falls monotonically when the channel bandwidth increases. In (Yanng, 1999), the dependence of the received signal level distribution on the channel bandwidth is studied by computer simulations, showing that the fade depth has a strong dependence on the equivalent channel bandwidth. In (Malik, 2008), a relationship between the fade depth and the channel bandwidth is derived from a measurements campaign carried out in an indoor scenario. Therefore, the study of the average signal level, the fade depth and the fade margin in wideband transmission systems is a key issue for the development of wireless systems. Since UWB systems employ a bandwidth higher than 500 MHz (FCC, 2002), an adequate characterization of the channel power variations is necessary to deploy such systems. In this section, we propose as a novel contribution an analytical approach to derive the fade depth and fade margin under the assumption that the received power is Gamma distributed. In our investigation, we have considered the IEEE 802.15.4a UWB channel model developed for indoor and outdoor environments in low data rate WPAN applications (Molisch, 2005), where the wireless channel is assumed quasi-static during the symbol transmission (Hashemi, 1993), the module of the channel impulse response of the UWB channel denoted by $|h(\tau)|=\alpha$, which describe the small scale fading in the time follow a Nakagami-*m* distribution, and the module of the channel transfer function $|H(f_i)|=r_i$ also follow a Nakagami-*m* distribution.

Since the module $|H(f_i)|$ of each of the frequency bins in a UWB channel can be approximated by a Nakagami-*m* distribution, then the instantaneous power in frequency follows a Gamma distribution (Nakagami-*m* squared). Therefore, it is possible to assume that the UWB channel power in a bandwidth $\Delta f = f_1 - f_2$, denoted by Ψ_f can be approximated by a Gamma distribution.

In the words, $r_i = |H(f_i)|$ represents the magnitude of the CTF and follows a Nakagami-*m* distribution, i.e., $r \sim \mathcal{M}(m_{eq}, \Omega_{eq})$, where m_{eq} is the fading parameter and Ω_{eq} the mean power in the frequency bin. $\Psi_f = r^2 = |H(f)|^2$ represents the power in a bandwidth $\Delta f = f_1 - f_2$, and follows a Gamma distribution, i.e. $\Psi_f \sim \mathcal{G}(m_{\Delta f}, \Omega_f)$. We have checked the results derived from this analytical approach with Monte Carlo simulation results for several environments described in the UWB IEEE 802.15.4a channel model.

2.4.1 Analytical approach of the power distribution in UWB channel: the Fade depth and the fade margin

In this section, we propose an analytical approach to evaluate the power distribution, the *fade depth* and the *fade margin* as a function of the channel bandwidth. This approach is based on the IEEE 802.15.4a channel model described previously. Asymptotic values for the *fade depth* and the *fade margin* are derived and compared with simulation results for indoor residential and outdoor environments in both line-of-sight (LOS) and non-line-of-sight (NLOS) conditions. Simulation results have been performed using the Monte Carlo method. For each environment considered, 1000 realizations of a small local area have been simulated, modeling the number of clusters, rays, cluster arrival and ray arrival times. The

small local area corresponds to a small region around the receiver, in which the number of clusters and rays are constant, and only the phase and amplitude of rays change for short displacements. In addition, for each realization, 60000 simulations of the MPCs phase and amplitude have been performed to model the power channel variations. Our analytical approach starts with the calculation of the channel transfer function (CTF) of the IEEE 802.15.4a UWB channel, this result was already found previously and is given by the Eq. (20) which is repeated here for convenience.

$$H(f_i) = \mathcal{F}\{h(\tau)\} = \sum_{l=1}^{L_C}\sum_{\substack{k=1 \\ l\neq k}}^{L_T} \alpha_{k,l} \exp\left\{-j\left[2\pi f_i\left(T_l + \tau_{k,l}\right) - \varphi_{k,l}\right]\right\} = \sum_{l=1}^{L_C}\sum_{\substack{k=1 \\ l\neq k}}^{L_T} \alpha_{k,l} \exp\left[-j\left(\theta_{k,l}\right)\right].$$

From the Parseval relation (Proakis, 1995), the UWB channel power in linear units (mW) inside the bandwidth, $\Delta f = f_2 - f_1$, denoted by $\Psi_{\Delta f}$, is calculated in frequency as

$$\Psi_{\Delta f} = \int_{f1}^{f2} \left|H(f)\right|^2 df, \tag{38}$$

where $|H(f)|$ is the magnitude of the CTF, f_1 and f_2 are the lower and upper frequencies, respectively. The squared module $|H(f)|^2$ is given according to (Llano et al., 2009) as

$$\left|H(f)\right|^2 = \left(\sum_{l=1}^{L_C}\sum_{k=1}^{L_T} \alpha_{k,l}^2 + \sum_{l=1}^{L_C}\sum_{\substack{n=1 \\ (l,k)\neq(n,m)}}^{L_C}\sum_{k=1}^{L_T}\sum_{m=1}^{L_T} \alpha_{k,l}\alpha_{m,n} \cos\left\{2\pi f\left[\left(T_l + \tau_{k,l}\right) - \left(T_n + \tau_{m,n}\right) + \left(\varphi_{k,l} - \varphi_{m,n}\right)\right]\right\} \right), \tag{39}$$

where $(l,k)\neq(n,m)$, represents the condition to evaluate the quadruple summation, i.e., $l\neq n$ OR $k\neq m$.

A. Channel power: We have assumed total independence between a pair of MPCs amplitude coefficients, in accordance with (Casioli et al., 2002), (Chong, 05) where the correlation coefficients between the amplitude of two MPCs measured remains below 0.2 (Casioli et al., 2002), and 0.35 (Chong, 2005). The UWB channel power inside the bandwidth Δf(Hz) according to Eq. (38) is given by

$$\begin{aligned} \Psi_{\Delta f}(\mathrm{mW}) = \int_{f1}^{f2} \left|H(f)\right|^2 df = \sum_{l=1}^{L_C}\sum_{k=1}^{L_T} \alpha_{k,l}^2 \int_{f1}^{f2} df + \\ \sum_{l=1}^{L_C}\sum_{\substack{n=1 \\ (l,k)\neq(n,m)}}^{L_C}\sum_{k=1}^{L_T}\sum_{m=1}^{L_T} \alpha_{k,l}\alpha_{m,n} \int_{f1}^{f2} \cos\left\{2\pi f\left[\left(T_l + \tau_{k,l}\right) - \left(T_n + \tau_{m,n}\right) + \left(\varphi_{k,l} - \varphi_{m,n}\right)\right]\right\} df \end{aligned}. \tag{40}$$

Solving the two integrals in Eq. (40), UWB channel power inside the bandwidth Δf(Hz), according to (Llano et al., 2010) is given by

$$\begin{aligned} \Psi_{\Delta f}(\mathrm{mW}) = \Delta f \sum_{l=1}^{L_C}\sum_{k=1}^{L_T} \alpha_{k,l}^2 + \\ \frac{1}{2\pi} \sum_{l=1}^{L_C}\sum_{\substack{n=1 \\ (l,k)\neq(n,m)}}^{L_C}\sum_{k=1}^{L_T}\sum_{m=1}^{L_T} \frac{\alpha_{k,l}\alpha_{m,n}}{\left(T_l + \tau_{k,l}\right) - \left(T_n + \tau_{m,n}\right)} \left[\sin\left(2\pi f_2 C_{l,n}^{k,m}\right) - \sin\left(2\pi f_1 C_{l,n}^{k,m}\right)\right] \end{aligned}, \tag{41}$$

where $C_{l,n}^{k,m} = \left[\left(T_l + \tau_{k,l}\right) - \left(T_n + \tau_{m,n}\right)\right] + \left(\varphi_{k,l} - \varphi_{m,n}\right)$. Note that in Eq. (40) the first term represents the average power inside the bandwidth Δf(Hz), and the second term the fluctuation of the instantaneous power as a function of the limits frequencies f_1 and f_2 and the delay of each multipath component. A comparison of the channel power PDF between simulated data and the Gamma approximation calculated using Eq. (41) for an indoor residential environment is shown in Fig. 10. The PDFs curves plotted correspond to a single realization (one small local area) of the indoor residential environment with LOS condition for different channel bandwidths (Δf = 2 GHz, 5 GHz, and 7 GHz).

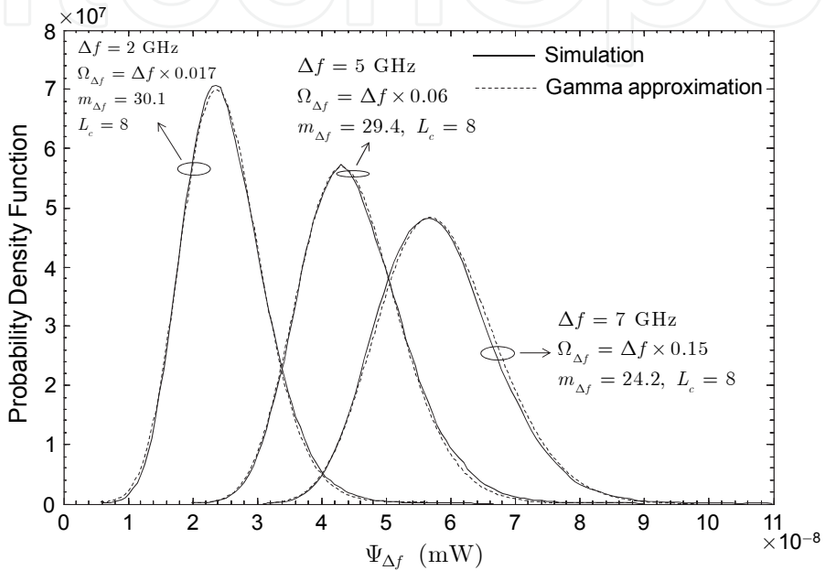

Fig. 10. Probability density function of the power, Ψ_f, in the indoor residential 802.15.4a UWB channel model with LOS condition and several values of channel bandwidth.

Other comparison that support the assumption that the Gamma distribution can be able to provide a good approximation to the channel power variations due to fast fading are shown in Fig. 11, where indoor residential and outdoor environments are considered in LOS and NLOS conditions with a channel bandwidth equal to 1 GHz. It is worth to note that the results show a higher fading parameter in LOS compared to the NLOS condition for the same channel bandwidth and environment. The parameters used in the simulation results are summarized in Table I. The goodness-of-fit of the Gamma distribution to the simulated data in Fig. 10 and Fig. 11 has been assessed through the Kolmogorov-Smirnov (KS) test for a 5% significant degree (Massey, 1951).

B. Mean power: The mean power denoted by Ω_f expressed in linear units (mW) in UWB channel inside of the bandwidth Δf can be calculated from Eq. (41) as

$$E\left\{\Psi_{\Delta f}\right\} = E\left\{\int_{f1}^{f2}\left|H\left(f\right)\right|^2 df\right\} = \Delta f \sum_{l=1}^{L_C}\sum_{k=1}^{L_T} E\left\{\alpha_{k,l}^2\right\} + \frac{1}{2\pi} \times \sum_{l=1}^{L_C}\sum_{\substack{n=1 \\ (l,k)\neq(n,m)}}^{L_C}\sum_{k=1}^{L_T}\sum_{m=1}^{L_T} E\left\{\frac{\alpha_{k,l}\alpha_{m,n}}{\left[\left(T_l + \tau_{k,l}\right) - \left(T_n + \tau_{m,n}\right)\right]}\left[\sin\left(2\pi f_2 C_{l,n}^{k,m}\right) - \sin\left(2\pi f_1 C_{l,n}^{k,m}\right)\right]\right\}. \quad (42)$$

Assuming the random variables $\alpha_{k,l}$, $\alpha_{m,n}$, $\varphi_{k,l}$, independents and the phase $\varphi_{k,l}$, uniformly distributed between 0 and 2π. Then, mean power for the IEEE 802.15.4a result to solve the Eq. (42) according to (Llano et al., 2010) as

$$\begin{aligned} E\left\{\Psi_{\Delta f}\right\} &= \Delta f \sum_{l=1}^{L_C}\sum_{k=1}^{L_T} E\left\{\alpha_{k,l}^2\right\} = \Delta f \sum_{l=1}^{L_C}\sum_{k=1}^{L_T} \Omega_{k,l} \\ &= \Delta f \sum_{l=1}^{L_C}\sum_{k=1}^{L_T} \exp\left[-\left(\frac{T_l}{\eta}+\frac{\tau_{k,l}}{\gamma}\right)\right] \times \frac{M_{\text{cluster}}}{\gamma\left[(1-\beta)\lambda_1+\beta\lambda_2+1\right]}. \end{aligned} \tag{43}$$

where $\Omega_{k,l}$ is the average power of each contribution in the 802.15.4a UWB channel calculated from the Eq. (16). Now, we investigate the channel power dependence on the channel bandwidth, deriving an analytical expression for the *fade depth* and the *fade margin*. Before performing these calculations is necessary to express the power of the UWB channel in logarithmic units (dBm) as $\Phi_{\Delta f}(\text{dBm})=10\log[\Psi_{\Delta f}(\text{mW})]$.

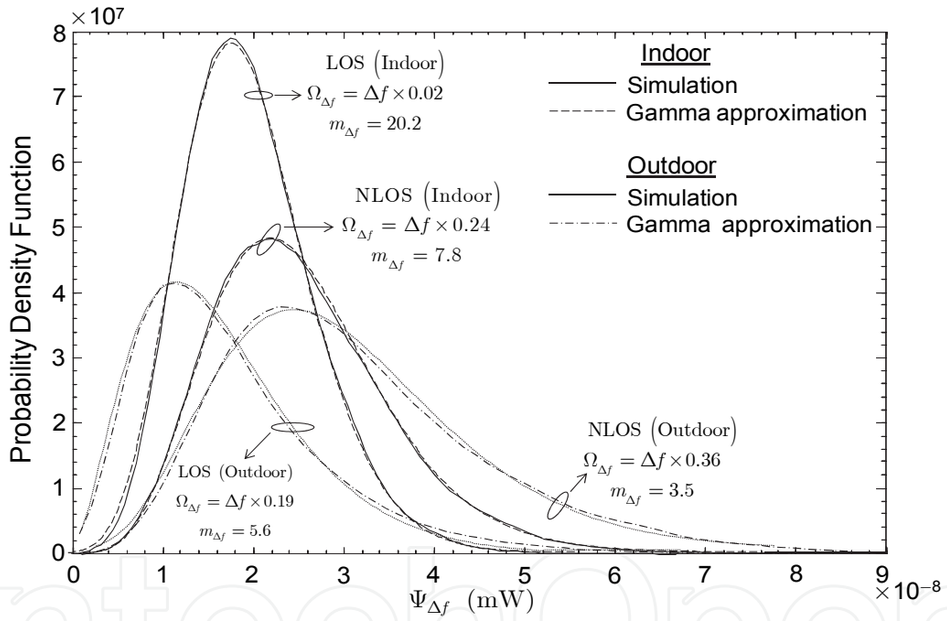

Fig. 11. Probability density function of the channel power, $\Psi\Delta f$, for indoor residential and outdoor environments with LOS and NLOS with a channel bandwidth Δf = 1 GHz.

C. Fade depth: The fade depth, denoted by $F_n\sigma$, can be defined as a measure of the channel power variation due to the small-scale fading (Malik, 2008). In a statistically sense, the fade depth is calculated as n times the standard deviation σ, of the channel power variations expressed in logarithmic units, i.e., $F_n\sigma = n\times\sigma$, with n = 1, 2, 3,…,. Therefore we calculated the standard deviation, σ, of channel power variation. Due to each MPC amplitude, $\alpha_{k,l}$, is modeled as a Nakagami-m random variable and the magnitude of the each frequency bin of the UWB channel $r=|H(f_i)|$ also is modeled as Nakagami-m distribution, according to the results show in Fig. 10 and Fig. 11, we have assumed that in a small local area around the receiver, the channel power variation $\Psi_f = r^2 = |H(f)|^2$ in linear units (mW) given by Eq. (41)

can be modeled as a Gamma distribution. As defined above the power of the UWB channel in logarithmic units (dBm) is expressed as $\Phi_{\Delta f}(\text{dBm})=10\log[\Psi_{\Delta f}(\text{mW})]$, the variance and standard deviation of the channel power in dBm is calculated as

$$\text{var}\left\{\Phi_{\Delta f}\left(\text{dBm}\right)\right\} \triangleq \sigma_{\Phi}^{2} = E\left\{\Phi_{\Delta f}^{2}\left(\text{dBm}\right)\right\} - E^{2}\left\{\Phi_{\Delta f}\left(\text{dBm}\right)\right\}. \tag{44}$$

Model parameters	Indoor residential		Outdoor	
	LOS	NLOS	LOS	NLOS
$\overline{L_c}$	3.0	3.5	13.6	10.5
Λ (1/ns)	0.047	0.12	0.0048	0.0243
λ_1 / λ_2 (1/ns)	1.54/0.15	1.77/0.15	0.13/2.41	0.15/1.13
β	0.095	0.045	0.0078	0.062
η (ns)	22.61	26.27	31.7	104.7
γ_0 (ns)	12.53	17.5	3.7	9.3
σ_{cluster} (dB)	2.75	2.93	3.0	3.0
k_γ	0	0	0	0
m_0 (dB)	0.67	0.69	0.77	0.56
k_m	0	0	0	0
$\hat{m}_0$ (dB)	0.28	0.32	0,78	0,25
$\hat{k}_m$	0	0	0	0

Table I. IEEE 802.15.4a UWB channel model parameters

The Gamma distribution in linear units can be derived easily from Nakagami-*m* distribution as, $r=\sqrt{\Psi}$, where Ψ and r are the RV Gamma and Nakagami-*m* respectively. Since cumulative distribution function (CDF) of RV Ψ (power) and r (amplitude) can be equal, i.e., $F_r(r) = F_\Psi(\Psi)$, then according to (Papoulis, 2002), (Peebles, 2001)

$$\int_{-\infty}^{r} f_X\left(x\right)dx = \int_{-\infty}^{\Psi} f_Y\left(y\right)dy\,. \tag{45}$$

Differentiating Eq. (45) and using transformation of variables, results

$$f_{\Psi}\left(\Psi\right) = f_r\left(r\right)\frac{dr}{d\Psi}\,. \tag{46}$$

The PDF of the Gamma distribution in linear units is obtained from Eq. (21) and Eq. (46) as

$$f_{\Psi\Delta f}\left(\Psi_{\Delta f}\right) = \frac{1}{\Gamma\left(m_{\Delta f}\right)}\left(\frac{m_{\Delta f}}{\Omega_{\Delta f}}\right)^{m\Delta f} \Psi_{\Delta f}^{\ m\Delta f-1}\exp\left(-\frac{m_{\Delta f}\Psi}{\Omega_{\Delta f}}\right),\ \Psi_{\Delta f}\geq 0,\ m_{\Delta f}\geq 0{,}5\,, \tag{47}$$

where, $\Psi_{\Delta f}$ (mW) is the power in the bandwidth Δf, $\Omega_{\Delta f} = E\{\Psi_{\Delta f}\}$ the average power, and $m_{\Delta f} = \Omega_{\Delta f}^2 \Big/ E\left\{\left(\Psi_{\Delta f} - \Omega_{\Delta f}\right)^2\right\}$ the fading parameter. As mentioned above the channel power in dBm, can be expressed as

$$\Phi_{\Delta f}\left(\text{dBm}\right) = 10\log\left(\Psi_{\Delta f}\right) \rightarrow \Psi_{\Delta f} = 10^{\frac{\Phi_{\Delta f}(\text{dBm})}{10}}. \tag{48}$$

From (48) perform the following transformations

$$\Phi_{\Delta f}\left(\text{dBm}\right) = \frac{10}{\ln(10)}\ln\left(\Psi_{\Delta f}\right); \quad \frac{\partial \Phi_{\Delta f}\left(\text{dBm}\right)}{\partial \Psi_{\Delta f}} = \frac{10}{\Psi_{\Delta f}\ln(10)}. \tag{49}$$

To solve Eq. (44) is necessary to express the Gamma distribution in dBm. From Eq. (46), Eq. (47) and Eq. (49), Gamma distribution in logarithmic units (dBm) is expressed as

$$f_{\Phi\Delta f}\left(\Phi_{\Delta f}\right) = \frac{\ln(10)}{10\Gamma\left(m_{\Delta f}\right)}\left(\frac{m_{\Delta f}}{\Omega_{\Delta f}}\right)^{m\Delta f} 10^{\frac{m\Delta f \Phi\Delta f}{10}} \exp\left(-\frac{m_{\Delta f}}{\Omega_{\Delta f}}10^{\frac{\Phi\Delta f}{10}}\right), \; -\infty < \Phi_{\Delta f} < \infty. \tag{50}$$

Variance and standard deviation of the power $\Phi_{\Delta f}$ (dBm) is calculated from the central moments of the Gamma random variable in dBm as

$$E\left\{\Phi_{\Delta f}^n\left(\text{dBm}\right)\right\} = \frac{\ln(10)}{10\Gamma\left(m_{\Delta f}\right)}\left(\frac{m_{\Delta f}}{\Omega_{\Delta f}}\right)^{m\Delta f} \int_{-\infty}^{\infty} \Phi_{\Delta f}^n 10^{\frac{m\Delta f \Phi\Delta f}{10}} \exp\left(-\frac{m_{\Delta f}}{\Omega_{\Delta f}}10^{\frac{\Phi\Delta f}{10}}\right) d\Phi_{\Delta f}. \tag{51}$$

Particularizing n = 1 in Eq. (51) and considering Eq. (48) and Eq. (49), we obtain the first moment of the Gamma RV in dBm as

$$E\left\{\Phi_{\Delta f}\left(\text{dBm}\right)\right\} = \frac{10}{\ln(10)\Gamma\left(m_{\Delta f}\right)}\left(\frac{m_{\Delta f}}{\Omega_{\Delta f}}\right)^{m\Delta f} \int_{0}^{\infty} \Psi_{\Delta f}^{m\Delta f - 1} \ln\left(\Psi_{\Delta f}\right) \exp\left(-\frac{m_{\Delta f}}{\Omega_{\Delta f}}\Psi_{\Delta f}\right) d\Psi_{\Delta f}. \tag{52}$$

To solve the integral in Eq. (50) we use (Gradshteyn, 2007, (4.352 1))

$$\int_0^{\infty} x^{\nu-1} \exp(-\mu x)\ln(x)\,dx = \frac{\Gamma(\nu)}{\mu^{\nu}}\left[\psi(\nu) - \ln(\mu)\right]; \; \text{Re}(\mu) > 0 \wedge \text{Re}(\nu) > 0, \tag{53}$$

where, $x = \Psi_{\Delta f}$, $\nu = m_{\Delta f}$, $\mu = m_{\Delta f}/\Omega_{\Delta f}$, $\Gamma(\cdot)$ gamma function and $\psi(\nu) = \frac{\partial}{\partial \nu}\left\{\ln\left[\Gamma(\nu)\right]\right\}$ Psi (digamma) function (Abramowitz, 1972, (6.3.1)). Therefore, the mean or first moment of the Gamma distribution in dBm can be expressed as

$$E\left\{\Phi_{\Delta f}\left(\text{dBm}\right)\right\} = \frac{10}{\ln(10)}\left[\psi\left(m_{\Delta f}\right) - \ln\left(\frac{m_{\Delta f}}{\Omega_{\Delta f}}\right)\right]. \tag{54}$$

The second central moment or mean squared value of the Gamma distribution is calculated by substituting in Eq. (51) n = 2, and using Eq. (49) is obtained

$$E\left\{\Phi_{\Delta f}^2\left(\mathrm{dBm}\right)\right\}=\left[\frac{10}{\ln(10)}\right]^2\frac{1}{\Gamma\left(m_{\Delta f}\right)}\left(\frac{m_{\Delta f}}{\Omega_{\Delta f}}\right)^{m\Delta f}\int_0^\infty \Psi_{\Delta f}^{m\Delta f-1}\left[\ln\left(\Psi_{\Delta f}\right)\right]^2\exp\left(-\frac{m_{\Delta f}}{\Omega_{\Delta f}}\Psi_{\Delta f}\right)d\Psi_{\Delta f}\,. \quad (55)$$

We can solve integral in Eq. (55) using (Gradshteyn, 2007, (4.358 2))

$$\int_0^\infty x^{\nu-1}\exp(-\mu x)\left[\ln(x)\right]^2dx=\frac{\Gamma(\nu)}{\mu^\nu}\left\{\left[\psi(\nu)-\ln(\mu)\right]^2+\zeta(2,\nu)\right\};\mathrm{Re}(\mu),\mathrm{Re}(\nu)>0, \quad (56)$$

where, $\zeta(\cdot,\cdot)$ Zeta Hurwitz function whose integral representation according to (WolframMathworld, 2011) is expressed as

$$\zeta(s,a)=\frac{1}{\Gamma(s)}\int_0^\infty\frac{t^{s-1}\exp(-at)}{1-\exp(-t)}dt;\ \ \mathrm{Re}(s)>1\wedge\mathrm{Re}(a)>0\,. \quad (57)$$

with $s = 2$ and $a = \nu$, according to (WolframMathworld_a, 2011), then $\zeta(a,\nu)$ is given by

$$\zeta(2,\nu)=\frac{1}{\Gamma(2)}\int_0^\infty\frac{t\exp(-\nu t)}{1-\exp(-t)}dt=\psi'(\nu), \quad (58)$$

Where $\psi'(\cdot)$ is trigamma function (Abramowitz, 1972 (6.4.1)) define the first derivate of digamma function or second derivate of the natural logarithm of gamma function. This is

$$\psi(\nu)=\frac{\partial}{\partial\nu}\left\{\ln\left[\Gamma(v)\right]\right\};\ \ \psi'(\nu)=\frac{\partial}{\partial\nu}\left[\psi(\nu)\right]=\frac{\partial^2}{\partial^2\nu}\left\{\ln\left[\Gamma(\nu)\right]\right\}. \quad (59)$$

Substituting Eq. (56) and Eq. (58) in Eq. (55) results (Llano et al., 2010)

$$E\left\{\Phi_{\Delta f}^2\left(\mathrm{dBm}\right)\right\}=\left[\frac{10}{\ln(10)}\right]^2\left\{\left[\psi\left(m_{\Delta f}\right)-\ln\left(\frac{m_{\Delta f}}{\Omega_{\Delta f}}\right)\right]^2+\psi'\left(m_{\Delta f}\right)\right\} \quad (60)$$

Finally, variance and standard deviation, σ, of the UWB channel power variation in dBm, is obtained by substituting Eq. (60) and Eq. (54) in Eq. (44), resulting according to (Llano et al., 2010)

$$\mathrm{var}\left\{\Phi_{\Delta f}\left(\mathrm{dBm}\right)\right\}=\left[\frac{10}{\ln(10)}\right]^2\psi'\left(m_{\Delta f}\right);\quad \sigma\left\{\Phi_{\Delta f}\left(\mathrm{dBm}\right)\right\}=\frac{10}{\ln(10)}\sqrt{\psi'\left(m_{\Delta f}\right)} \quad (61)$$

Note, that the standard deviation, σ, does not depend on the mean power $\Omega_{\Delta f}$, but depends on the fading parameter $m_{\Delta f}$, defined as

$$m_{\Delta f}=\frac{\left(E\left\{\Psi_{\Delta f}\right\}\right)^2}{E\left\{\left(\Psi_{\Delta f}\right)^2\right\}-\left(E\left\{\Psi_{\Delta f}\right\}\right)^2} \quad (62)$$

The numerator of Eq. (62) correspond to the mean power calculated in Eq. (43) square, i.e.,

$$\left(E\left\{\Psi_{\Delta f}\right\}\right)^2 = \left(\Delta f \sum_{l=1}^{L_C}\sum_{k=1}^{L_T}\Omega_{k,l}\right)^2 \tag{63}$$

Calculating, $E\{(\Psi_{\Delta f})^2\}$ using Eq. (41) results

$$E\left\{\left(\Psi_{\Delta f}\right)^2\right\} = (\Delta f)^2\left(\sum_{l=1}^{L_C}\sum_{k=1}^{L_T}E\left\{\alpha_{k,l}^4\right\} + \sum_{l=1}^{L_C}\sum_{\substack{k=1\\k\neq l}}^{L_T}\sum_{n=1}^{L_C}\sum_{\substack{m=1\\m\neq n}}^{L_T}E\left\{\alpha_{k,l}^2\right\}E\left\{\alpha_{m,n}^2\right\}\right) + \\ + \frac{1}{2\pi^2}\sum_{l=1}^{L_C}\sum_{\substack{k=1\\k\neq l}}^{L_T}\sum_{n=1}^{L_C}\sum_{\substack{m=1\\m\neq n}}^{L_T}\frac{E\left\{\alpha_{k,l}^2\right\}E\left\{\alpha_{m,n}^2\right\}}{\left[\left(T_l+\tau_{k,l}\right)-\left(T_n+\tau_{m,n}\right)\right]^2}\times D_{l,n}^{k,m} \tag{64}$$

where $D_{l,n}^{k,m} = \sin^2\left\{\pi\Delta f\left[\left(T_l+\tau_{k,l}\right)-\left(T_n+\tau_{m,n}\right)\right]\right\}$, $(l,k)\neq(n,m)$ represents the condition to evaluate the quadruple summation, i.e., $l\neq n$ OR $k\neq m$. Substituting Eq. (63) and Eq. (64) in Eq. (62) and after some mathematical operations, results

$$m_{\Delta f} = \frac{\left(\Delta f\sum_{l=1}^{L_C}\sum_{k=1}^{L_T}\Omega_{k,l}\right)^2}{(\Delta f)^2\sum_{l=1}^{L_C}\sum_{k=1}^{L_T}\frac{\Omega_{k,l}^2}{m_{k,l}} + \frac{1}{2\pi^2}\sum_{l=1}^{L_C}\sum_{\substack{n=1\\(l,k)\neq(n,m)}}^{L_C}\sum_{k=1}^{L_T}\sum_{m=1}^{L_T}\frac{\Omega_{k,l}\Omega_{m,n}}{\left[\left(T_l+\tau_{k,l}\right)-\left(T_n+\tau_{m,n}\right)\right]^2}\times D_{l,n}^{k,m}}, \tag{65}$$

where $\Omega_{k,l}$, $m_{k,l}$, T_l and $\tau_{k,l}$, are defined according to UWB channel model. As defined above the fade depth can be calculated as n times the standard deviation, σ, of the channel power variations in dBm, i.e., $F_{n\sigma} = n\times\sigma$, with n = 1, 2, 3,…,. Thus, the fade depth is analytically calculated as

$$F_{n\sigma}(\mathrm{dB}) = \frac{10n}{\ln(10)}\sqrt{\psi'\left(m_{\Delta f}\right)}\,. \tag{66}$$

Trigamma function $\psi'(\cdot)$ can be evaluated numerically using Mathematica®, or Matlab®. However, this function can also be expressed using an equivalent function. For values of $m_{\Delta f} \geq 1$, the trigamma function, according to (Abramowitz, 1972, (6.4.12)) is approximated by an asymptotic series expansion. Therefore, the fade dept is expressed as

$$F_{n\sigma}(\mathrm{dB}) = \frac{10n}{\ln(10)}\sqrt{\psi'\left(m_{\Delta f}\right)} \cong \frac{10n}{\ln(10)}\sqrt{\frac{1}{m_{\Delta f}}+\frac{1}{2m_{\Delta f}^2}+\frac{1}{6m_{\Delta f}^3}} \tag{67}$$

The relative error of Eq. (67) series expansion is less than 6.6×10^{-3} for $m_{\Delta f} \geq 1$, which corresponds to the values used in simulations. A comparison between the analytical approximation of the fade depth given by Eq. (67) and simulation results is shown in Fig. 12 for an indoor residential environment with NLOS condition. The channel parameters used in the simulation results are summarized in Table I. It can be observed that simulation and analytical results are very similar, which is in agreement with the assumption that the power in a channel bandwidth Δf can be modeled by a Gamma distribution.

The results also show that in channel bandwidths less than 1 MHz (Narrowband channel), the fade depth $F_{n\sigma}$ is approximately constant: 5.6 dB for n = 1, 11.0 dB for n = 2, 16.5 dB for

n = 3 and 27.8 dB for n = 5, as corresponds to the behavior of a narrowband channel without frequency diversity gain. From Fig. 12 we can also observe that $F_{n\sigma}$ converges asymptotically from approximately 2 GHz. Note that the fade depth is lower in UWB channels (0.8 dB for n = 1) which narrowband channels (5.6 dB for n = 1), this mean the UWB systems are more resistant to multipath. The floor level of the fade depth is a consequence of the amplitude variations of the MPCs for short displacements of the receiver within a small local area. The maximum error between simulation and analytical results is approximately 0.45 dB for n = 1, corresponding to Δf = 8 MHz.

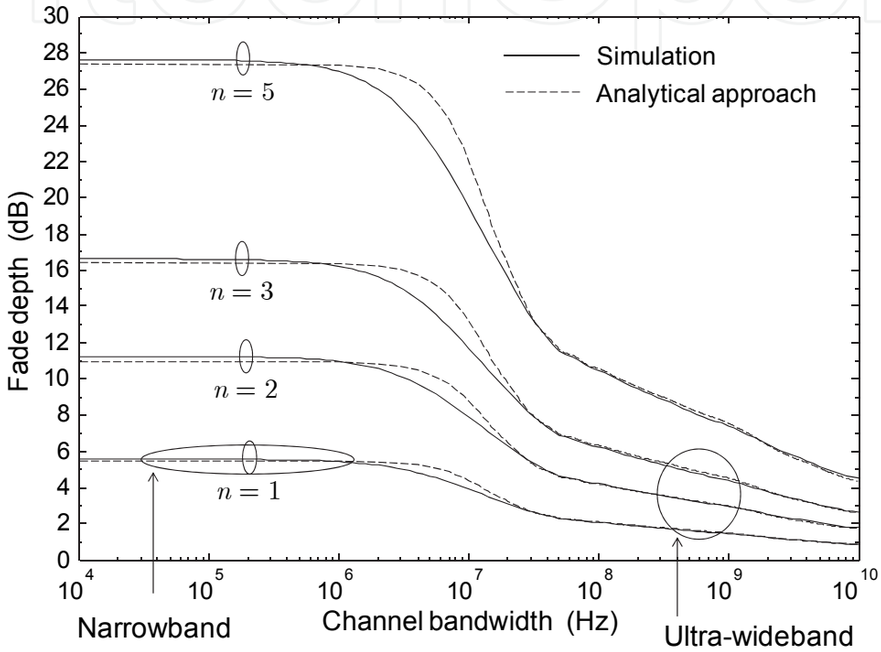

Fig. 12. Fade depth, $F_{n\sigma}$, for the indoor residential IEEE 802.15.4a UWB channel model derived from the analytical approach and simulation results under NLOS condition.

C. Fade margin: The fade margin can be defined as the difference in channel power corresponding to a probability P and the 50% of the cumulative distribution function (CDF) of the received channel power (Fig. 13). The fade margin associated to a probability P and denoted by FM_P , is related to the channel power by

$$P = \Pr\left\{E\left\{\Phi_{\Delta f}\left(\text{dBm}\right)\right\} - FM_{P\%}\left(\text{dB}\right) \le \Phi_{P\%}\left(\text{dBm}\right)\right\}, \tag{68}$$

where, $\Phi_{\Delta f}$(dBm) is the channel power in dBm calculated from Eq. (41) in a bandwidth Δf, as $\Phi_{\Delta f}$(dBm)=10log[$\Psi_{\Delta f}$(mW)], and $\Phi_{P\%}$(dBm) is the channel power not exceeded with a probability P%.

Average channel power in dBm denoted by $E\{\Phi_{\Delta f}(\text{dBm})\}$ was calculated in Eq. (54). The value not exceeded with a probability P% of a Gamma RV in logarithmic units, $\Phi_{P\%}$ (dBm) whose PDF given by Eq. (50), is expressed as $P = \text{Prob}\left\{\Phi_{\Delta f} \le \Phi_P\right\}$. For convenience, we calculate this probability using the PDF of the corresponding Gamma distribution as

$$P = \text{Prob}\left\{\Phi_{\Delta f} \le \Phi_P\right\} = \text{Prob}\left\{\Psi_{\Delta f} \le \Psi_P\right\} = \int_0^{\Psi_P} f_{\Psi\Delta f}\left(\Psi_{\Delta f}\right) d\Psi_{\Delta f}\,, \tag{69}$$

where, $f_{\Psi\Delta f}\left(\Psi_{\Delta f}\right)$ is the PDF of the Gamma RV in linear units given by Eq. (47). Substituting Eq. (47) in Eq. (69) results

$$P = \frac{1}{\Gamma\left(m_{\Delta f}\right)}\left(\frac{m_{\Delta f}}{\Omega_{\Delta f}}\right)^{m\Delta f} \int_0^{\Psi_P} \Psi_{\Delta f}^{\;m\Delta f-1} \exp\left(-\frac{m_{\Delta f}\Psi_{\Delta f}}{\Omega_{\Delta f}}\right) d\Psi_{\Delta f}\,,\ \Psi_{\Delta f} \ge 0,\ m_{\Delta f} \ge 0{,}5\,. \tag{70}$$

Solving the integral in Eq. (70) is obtained

$$P = 1 - \frac{1}{\Gamma\left(m_{\Delta f}\right)}\Gamma\left(m_{\Delta f}, \frac{m_{\Delta f}}{\Omega_{\Delta f}}\Psi_P\right), \tag{71}$$

where $\Gamma(\cdot,\cdot)$ is the incomplete function gamma (Abramowitz, 1972, (6.5.3)). Since our objective is to calculate Ψ_P, which is inside argument of incomplete function gamma, we use the regularized incomplete function gamma $Q(\cdot,\cdot)$ defined according to (WolframMathworld_b, 2011) as

$$z = Q\left(a,s\right) = \frac{\Gamma\left(a,s\right)}{\Gamma\left(a\right)}\,, \tag{72}$$

where $a = m_{\Delta f}$, $s = m_{\Delta f}\Psi_P/\Omega_{\Delta f}$, and $z = 1-P$. Operating on Eq. (72) according to Eq. (71) and using the inverse of the regularized incomplete function gamma $Q^{-1}(\cdot,\cdot)$ defined in (WolframMathworld_c, 2011) as

$$z = Q\left(a,s\right)/;\rightarrow s = Q^{-1}\left(a,z\right) \tag{73}$$

After carry out simple mathematical operation in Eq. (73), power $\Psi_{P\%}$ in linear units (mW) not exceeded with a probability P% is given according to (Llano et al., 2010) as

$$\Psi_P\left(\text{mW}\right) = \frac{\Omega_{\Delta f}}{m_{\Delta f}} Q^{-1}\left(m_{\Delta f}, 1-P\right) \tag{74}$$

Expressing Eq. (74) in logarithmic units (dBm), results

$$\Phi_P\left(\text{dBm}\right) = 10\log\left[\Psi_P\left(\text{mW}\right)\right] = 10\log\left(\frac{\Omega_{\Delta f}}{m_{\Delta f}}\right) + 10\log\left[Q^{-1}\left(m_{\Delta f}, 1-P\right)\right], \tag{75}$$

Finally we can obtain a closed form expression of the fade margin FM_P(dB) for UWB channel substituting Eq. (54) and Eq. (75) in Eq. (68), resulting

$$FM_P\left(\text{dB}\right) = \frac{10}{\ln\left(10\right)}\psi\left(m_{\Delta f}\right) - 10\log\left[Q^{-1}\left(m_{\Delta f}, 1-P\right)\right]. \tag{76}$$

where $m_{\Delta f}$ is given by Eq. (65). Note that the fade margin is independent of the mean channel power $\Omega_{\Delta f}$. For P approximating to 0, the regularized incomplete Gamma function

Q^{-1} can be asymptotically extended according to (WolframMathworld_d, 2011). Therefore, the fade margin given by Eq. (76) can be written as

$$FM_P(\mathrm{dB})_{P\to 0} \cong \frac{10\psi\left(m_{\Delta f}\right)}{\ln(10)} - 10\log\left\{\omega^1 + \frac{\omega^2}{\left(m_{\Delta f}+1\right)} + \frac{\left(3m_{\Delta f}+5\right)\omega^3}{2\left(m_{\Delta f}+1\right)^2\left(m_{\Delta f}+2\right)} + \frac{\left[m_{\Delta f}\left(8m_{\Delta f}+33\right)+31\right]\omega^4}{3\left(m_{\Delta f}+1\right)^3\left(m_{\Delta f}+2\right)\left(m_{\Delta f}+3\right)} + \cdots\right\}, \quad (77)$$

where $\omega = \left[\Gamma\left(m_{\Delta f}+1\right)P\right]^{\frac{1}{m_{\Delta f}}}$. We have found that the error using Eq. (77) increases as $m_{\Delta f}$. For a relative error between the closed form expression given by Eq. (76) and the approximation given by Eq. (77) equal to 1%, for 6 terms of the summation, the maximum value of $m_{\Delta f}$ is 9.9 for a probability P = 1% and 15.6 for a probability P = 0.1%.

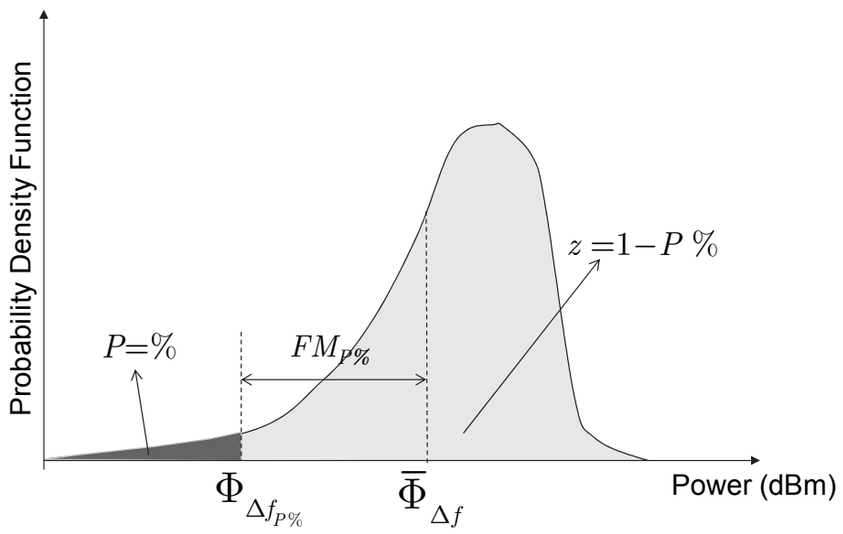

Fig. 13. Fade margin in UWB channel

Fig. 14 shows the fade margin FM_p given by Eq. (76) for the indoor residential NLOS 802.15.4a channel model as a function of the channel bandwidth for three different probabilities: P = 5%, 10% and 20%. Note that the fade margin in a channel bandwidth less than 1 MHz is approximately constant, and the difference between the Gamma approximation and the simulation for these bandwidth values is around 0.05 dB for P = 20%, 0.05 dB for P = 10%, and 0.25 dB for P = 5%. Moreover, a maximum difference of 1 dB and 0.5 dB between the Gamma approximation and simulation results is found at Δf = 8 MHz, for P = 5% and P = 10%, respectively.

The difference between analytical and simulation results in Fig. 14 can be explained analyzing the second term of the channel power given by Eq. (41). For high channel bandwidths, the second term in Eq. (41) is negligible compared to the first term. Thus, the channel power in linear units (mW) can be approximated as a Gamma distribution. For low channel bandwidths, the second term in Eq. (41) corresponds to the finite sum of $\alpha_{k,l}\alpha_{m,n}$,

where $\alpha_{k,l}$ and $\alpha_{m,n}$ are Nakagami-*m* distributed and mutually independent RVs. It can be demonstrated that the sum of the product of Nakagami-*m* RVs can be approximated as a Gamma distribution (Nakagami, 1960). Therefore, the channel power is well approximated as a Gamma distribution. Nevertheless, for medium channel bandwidths, between 2 MHz and around 50 MHz for the results shown in Figure 14, the channel power in linear units is not approximated so well to a Gamma distribution due to the second term in Eq. (41).

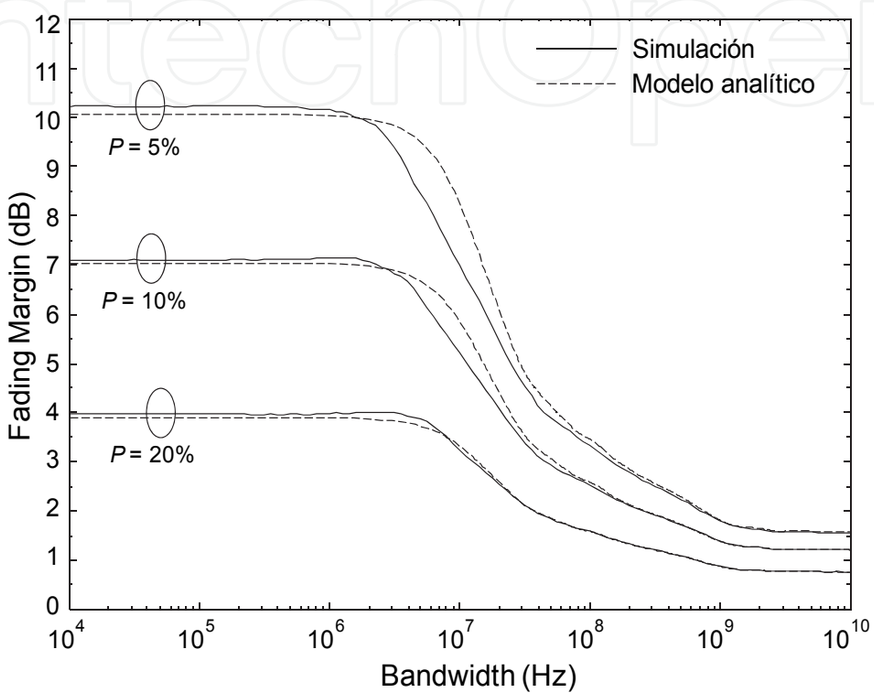

Fig. 14. Fade margin, FM_P, in the indoor residential IEEE 802.15.4a UWB channel model derived from the analytical approach and simulation results in NLOS condition.

3. Conclusions

In this chapter, we showed that UWB channel with small-scale fading statistics modeled as lognormal or Nakagami-*m* RV can be approximated in the frequency domain by a Nakagami-*m* distribution, whose fading and mean power parameters are explicit functions of the delay parameters and decay time constants of the UWB channel. Moreover the subcarrier frequency distribution can be approximated by a Rayleigh distribution if the number of MPC is high. Additionally, we found an exact expression for the correlation coefficient between a couple of subcarriers amplitudes in the frequency for the IEEE 802.15.3a and IEEE 802.15.4a UWB channel.

Also, we investigate the variations of the received power as a function of the bandwidth channel, taking the IEEE 802.15.4a channel model as our point of reference. The results show that the channel power can be modeled by a Gamma distribution. Under the assumption that the channel power is Gamma distributed, an analytical approach to characterize the *fade depth* and the *fade margin* for indoor and outdoor environments is proposed. Also, asymptotic expressions for the fading parameter of the Gamma distribution as a function of

the channel rms delay spread are proposed and discussed. The performance of the analytical approach has been checked by comparison with simulation results considering different propagation conditions for indoor residential and outdoor environments. The results show that the fade depth is approximately constant for channel bandwidths below 1 MHz (just about 5.5 dB for n=1), i.e, the fade depth is bandwidth independent for narrowband channels, and adopts an asymptotic convergence for channel bandwidths beyond 2 GHz (just about 0.8 dB for n=1). A similar behavior of the fade margin occurs in terms of the channel bandwidth. This analytical approach enables a proper evaluation of the link budget in terms of the bandwidth channel and it can be used to design and implement UWB communications systems.

4. References

Abramowitz M, I.A., Stegun. (1972). Handbook of Mathematical Functions; with Formulas, Graphs and Mathematical Tables.

Batra A, J. Balakrishnan, G. R. Aiello, J. R, Foerster, & A. Dabak. (2004). Design of a multiband OFDM system for realistic UWB channel environments. *IEEE Trans. Microwave Theory Tech.*, vol. 52, no. 9, pp. 2123-2138.

Bastidas-Puga E.R, F. Ramírez-Mireles, & D. Muñoz-Rodríguez. (2005). On fading margin in ultra wideband communications over multipath channels. *IEEE Transactions on Broadcasting*, vol. 51, pp. 366-370, Sep. 2005.

Cardoso F. & L. Correia. (2003). Fading depth dependence on system bandwidth in mobile communications – an analytical approximation. *IEEE Trans. Veh. Technol.*, vol. 52, pp. 587-593, May 2003.

Cassioli D, M. Z. Win, & A.F. Molisch. (2002). The ultra-wideband indoor channel: from statistical model to simulations. *IEEE J. Select. Areas Commun.*, vol. 20, pp. 1247-1252.

Chong C.C, & S. K. Yong. (2005). A generic statistical-based UWB channel model for high-rise apartments. *IEEE Trans. Antennas Propag.*, vol. 53, no. 8, pp. 2389–2399.

Díaz A, A.P. García, L. Rubio. (2007). Time dispersion characterization for UWB mobile radio channels between 3.1 and 10.6 GHz. *IEEE Proc. Int. Symp. Antennas and Propagation Society*, Hawaii, USA, June, 2007.

European Committee for Standardization. (2007). Standardization mandate forwarded to cen/cenelec/etsi for harmonised standards covering ultra-wideband equipment. [Online]. Available: http://www.etsi.org/WebSite/document/aboutETSI/EC_Mandates/m407_EN_Adonis_13099.pdf

Fleury B.H. (1996). An uncertainty relation for WSS processes and its application to WSSUS systems. *IEEE Trans. Commun.*, vol. 44, no. 12, pp. 1632-1634.

Federal Communications Commission. (2002). Revision of part 15 of the commission´s rules regarding ultra-wideband transmission systems: first report and order. Federal Communications Commission, USA, Washington, DC, USA, Tech. Rep. FCC 02-48, February 2002

Foerster J.R *et al*. (2002). Channel modeling subcommittee final report. IEEE, Document IEEE 02490r0P802-15 SG3a, 2003.

Gradshteyn I.S & I.M. Ryzhik. (2007). Tables of Integrals, Series and Products. Nueva York: Academic, 2007.

Hashemi H. (1993). Impulse response modeling of indoor radio propagation channels. *IEEE J. Select. Areas Commun*., vol. 11, pp. 967–978.

Jakes W.C. (1974), *Microwave Mobile Communications*. Wiley, New York, 1974.

Liuqing Y, & G.B. Giannakis. (2004). Ultra-wideband communications: an idea whose time has come. *IEEE Signal Processing Mag*., vol. 21, pp. 26-54, Nov. 2004.

Llano G. J. Reig, & L. Rubio. (2009). The UWB-OFDM channel analysis in frequency. *IEEE 69th Vehicular Technology Conference*: VTC2009-Spring 26–29-. Barcelona, Spain.

Llano G. Reig, J. Rubio, L. (2010). Analytical Approach to Model the Fade Depth and the Fade Margin in UWB Channels. *IEEE Trans. Veh. Technol*., vol. 48, no. 9, pp. 4214-4221.

Massey F.J. (1951). The Kolmogorov-Smirnov test for goodness of fit. *Journal of the American Statistical Association*, vol. 46, no. 253, pp. 68-78, 1951.

Molish A. F. *et al*,. (2005). IEEE 802.15.4a channel model final report. Tech. Rep., Document IEEE 802.1504-0062-02-004a.

Molisch A.F. (2005). Ultra wideband propagation channels theory, measurement, and modeling. *IEEE Trans. on Veh. Technol*., vol. 54, pp. 1528-1545, Sep. 2005.

Malik W.Q. B. Allen, & D.J. Edwards (2008). Bandwidth dependent modeling of small scale fade depth in wireless channels. *IET Microw. Antenn. Propag*., vol. 2, no. 6, pp. 519-528.

Nakagami M. (1960). The *m*-distribution, a general formula of intensity distribution of rapid fading," *in Statistical Methods of Radio Wave Propagation*, W. G. Hoffman, Ed. Oxford, England.

Papoulis A. & Unnikrishna S. (2002). *Probability, Random Variables and Stochastic Processes*. 4th ed. New York: McGraw-Hill.

Proakis J. G. (1995). *Digital Communications*. Third Edition, McGraw-Hill Book Company, New York.

Peebles P.Z, Jr. (2001). *Probability, Random Variables and Random Signal Principles*. 4th ed. New York: McGraw-Hill.

Rappaport T.S. (1996). Wireless Communications Principles and Practice, Prentice Hall, Inc, New Jersey.

Saleh A.M. & R. Valenzuela. (1987). A statistical model for indoor multipath propagation. *IEEE J. Select. Areas Commun*, vol 2, pp. 128-137.

WolframMathworld. (2011, Feb). [Online]. Available:
http://functions.wolfram.com/10.02.07.0001.01 (Last access, 15/02/2011)

WolframMathworld. (2011, Feb). [Online]. Available:
http://functions.wolfram.com/10.02.03.0029.01 (Last access, 15/02/2011)

WolframMathworld. (2011, Feb). [Online]. Available:
http://functions.wolfram.com/06.08.02.0001.01 (Last access, 15/02/2011)

WolframMathworld. (2011, Feb). [Online]. Available:
http://functions.wolfram.com/06.12.02.0001.01 (Last access, 15/02/2011)

WolframMathworld. (2011, Feb). [Online]. Available:
http://functions.wolfram.com/06.12.06.0007.01 (Last access, 15/02/2011)

Yang J. & S. Kozono. (1999). A study of received signal-level distribution in wideband transmissions in mobile communications. *IEEE Trans. Veh. Technol*., vol. 48, pp. 1718-1725.

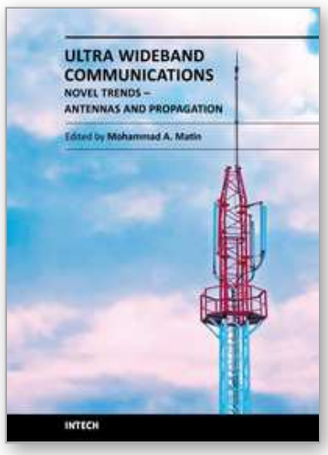

Ultra Wideband Communications: Novel Trends - Antennas and Propagation

Edited by Dr. Mohammad Matin

ISBN 978-953-307-452-8
Hard cover, 384 pages
Publisher InTech
Published online 09, August, 2011
Published in print edition August, 2011

This book explores both the state-of-the-art and the latest achievements in UWB antennas and propagation. It has taken a theoretical and experimental approach to some extent, which is more useful to the reader. The book highlights the unique design issues which put the reader in good pace to be able to understand more advanced research.

How to reference

In order to correctly reference this scholarly work, feel free to copy and paste the following:

Gonzalo Llano, Juan C. Cuellar and Andres Navarro (2011). Frequency UWB Channel, Ultra Wideband Communications: Novel Trends - Antennas and Propagation, Dr. Mohammad Matin (Ed.), ISBN: 978-953-307-452-8, InTech, Available from: http://www.intechopen.com/books/ultra-wideband-communications-novel-trends-antennas-and-propagation/frequency-uwb-channel

INTECH
open science | open minds

InTech Europe
University Campus STeP Ri
Slavka Krautzeka 83/A
51000 Rijeka, Croatia
Phone: +385 (51) 770 447
Fax: +385 (51) 686 166
www.intechopen.com

InTech China
Unit 405, Office Block, Hotel Equatorial Shanghai
No.65, Yan An Road (West), Shanghai, 200040, China
中国上海市延安西路65号上海国际贵都大饭店办公楼405单元
Phone: +86-21-62489820
Fax: +86-21-62489821

IntechOpen